

Synthesis and Characterization of Transparent and Conducting Thin Films



A thesis submitted towards partial fulfilment of
BS-MS Dual Degree Programme

by

RASHMI RUNJHUN

under the guidance of

DR. SULABHA K. KULKARNI

UGC Professor

INDIAN INSTITUTE OF SCIENCE EDUCATION AND RESEARCH
PUNE

Certificate

This is to certify that this thesis entitled “*Synthesis and Characterization of Transparent and Conducting Thin films*” submitted towards the partial fulfilment of the BS-MS dual degree programme at the Indian Institute of Science Education and Research (IISER) Pune represents original research carried out by **Rashmi Runjhun** at IISER Pune, under the supervision of **Prof. Sulabha K. Kulkarni** during the academic year 2013-2014.

Rashmi Runjhun
20091065

Sulabha K. Kulkarni
UGC Professor

Acknowledgments

I would like to express my sincere gratitude to my mentor Prof. Sulabha K. Kulkarni for the continuous support in my MS final year project, for her patience, motivation, enthusiasm, and immense knowledge. Her valuable guidance has helped me in all the time of research and writing of this thesis. I have learnt a lot from her and it will be greatly useful for me in the future. Besides my mentor, I would also like to thank Dr. Smita Chaturvedi for her helpful suggestions.

Also, I thank my lab members Amey and Prashant for being a great support throughout my project, their advices, encouragement as well as making the atmosphere of the lab lively. I thank my other lab members Abhijit, Jensheer and Bhuneshwar for their cooperation. I also thank my friends for being there and helping me in every possible manner.

Furthermore, I also thank Mr. Anil Prathamshetti for his technical assistance in FESEM and helping me in obtaining useful data for this project. I thank Dr. Mrinalini Puranik and Mr. Sayan Modal for the help in recording Raman spectra in their lab.

I would like to thank all those who are affiliated to IISER Pune for their direct and indirect support.

Last but not the least, I thank my family for believing in me and fulfilling all my needs throughout my life, without which I would not have come this far.

Abstract

Transparent and conducting thin films (TCFs) have turned out to be the materials which are applicable in diverse areas in modern technology. These are the materials which should be electrically conducting as well as transparent in the visible region. These properties make them suitable to be used in various displays, electromagnetic interference shielding, solar cells, as energy efficient coatings and so on. However the most popular material for presently used TCFs, indium doped tin oxide (ITO) needs a replacement because of its toxicity, high price and scarcity. These drawbacks have resulted in the search of other materials which can serve as the alternatives for ITO. Organic films made from graphene, reduced graphene oxide or carbon nanotubes and metallic nanofilms are being explored for this purpose.

This project was intended to prepare TCFs using graphene oxide (GO), gold nanowires (Au NWs) as well as a hybrid of these two. Large area GO films were prepared following the eco-friendly and very simple hydrothermal method using sugars. Films with varying thicknesses were also synthesized by changing the reaction parameters. Characterization techniques such as Field Emission Scanning electron microscope (FESEM), Atomic force microscope (AFM), UV-Vis spectroscopy, Fourier transform infrared spectroscopy (FTIR) and Raman spectroscopy were used to study the properties of these films. Reduction of GO was carried out by a combination of chemical and thermal reduction. Au NWs were also synthesized by a very simple and one-step wet chemical method and were later characterized by the FESEM and UV-Vis spectroscopy. In addition, hybrid films were prepared and characterized by FESEM. Later, transparency measurements by solid state UV-Vis spectrophotometer revealed that GO and Au NWs films had different transparencies depending upon the thickness of the films. For wavelength in range 400-800nm, transparency up to 90% was achieved for GO films and 97% for Au NWs films. The conductivity measurement showed that as prepared GO was an insulator. However, the reduction process decreased its sheet resistance by two orders. The Au NWs films also had high sheet resistance because of the capping agents attached and due to the contact resistance between the wires. The conductivity and transparency measurements for the hybrid film are in progress. In the near future, the plan is to optimize the properties of these films for better results.

Contents

1	Introduction	3
1.1	Transparent and Conducting Thin Films (TCFs)	3
1.1.1	Applications of TCFs	5
1.2	Need For the Replacement of TCOs	6
1.3	Graphene	6
1.4	Graphene Oxide (GO)	8
1.4.1	Synthesis of GO	9
1.4.2	Reduction of GO	11
1.5	Gold Nanowires (AuNWs)	12
1.5.1	Optical Properties of Au NWs	12
1.5.2	Synthesis of Au NWs	13
1.6	Summary	14
1.7	Bibliography	14
2	Experimental Methods and Techniques	17
2.1	Synthesis Methods	17
2.1.1	Hydrothermal Synthesis of GO	17
2.1.2	Reduction of GO	18
2.1.3	Synthesis of Au NWs	18
2.1.4	Synthesis of GO/Au NWs Composite	18
2.2	Characterization Techniques	19
2.2.1	UV-Vis Spectroscopy	19
2.2.2	Scanning Electron Microscope (SEM)	20
2.2.3	Atomic Force Microscope (AFM)	21
2.2.4	Fourier Transform Infrared Spectroscopy (FTIR)	22
2.2.5	Raman Spectroscopy	23
2.2.6	Four-Point Probe Method	25
2.3	Bibliography	26
3	Results and Discussions	27
3.1	Graphene Oxide (GO)	27
3.1.1	AFM analysis	29
3.1.2	SEM analysis	31
3.1.3	FTIR analysis	32
3.1.4	Raman analysis	33
3.2	Reduction of GO	34
3.2.1	FTIR analysis	34
3.2.2	Raman analysis	35

3.3	Gold Nanowires (Au NWs)	36
3.3.1	SEM analysis	37
3.3.2	UV-Vis absorption analysis	38
3.4	Hybrid film of GO/Au NWs	39
3.5	Transparency measurements of films	41
3.6	Conductivity measurement of films	42
3.7	Summary	43
3.8	Bibliography	44
4	Conclusions and Future Directions	45

Chapter 1

Introduction

Nanoscience has revolutionized modern technology. It has emerged as a whole new and extremely interesting subject in the last few decades. As the name suggests, this field includes the study of materials having size range of ~ 1 to 100nm ($1\text{nm} = 10^{-9}\text{m}$). At such small scales, lots of interesting phenomena start to occur. The mechanical, thermal, optical, magnetic and other properties show different trends as compared to bulk materials. So, for the same material, different properties can be achieved just by changing their size. For instance, bulk gold has bright yellow colour but the solution of gold nanowires show light pink colour.

Nanomaterials can have various shapes or morphology. They can be 0D (quantum dots), 1D (nanowires), 2D (nanofilms), 3D (nanospheres, nanorods, and other shapes). In this chapter, more will be discussed about the nanofilms. In the first part, overview of transparent and conducting films and their applications will be given. Later, the need for the replacement of currently used transparent conducting oxides will be discussed. Subsequent sections will be focused on the properties of graphene oxide and Gold nanowires, which I have used for the synthesis of transparent and conducting films as an alternative for the traditional materials used.

1.1 Transparent and Conducting Thin Films (TCFs)

TCFs are essential in current world of technology. Such materials should have large optical transparency as well as electrical conductivity in thin layers. Because of these properties, they would be applicable to a wide variety of areas. The applications of these TCFs will be discussed in detail in later section. A statistical data indicates that the research in the area of TCFs is increasing rapidly year by year as shown in the fig. 1.1.

A combination of transparency and conduction can be achieved in different types of materials. There are basically three types of TCFs as discussed below

1) Inorganic – These films are typically made from the transparent and conducting oxides (TCO). Their resistivity could be as low as $10^{-4}\Omega\text{cm}$ [1]. The resistivity of any material is the opposition in the flow of electric current by the material and given by the formula

$$\rho = R \frac{A}{L}$$

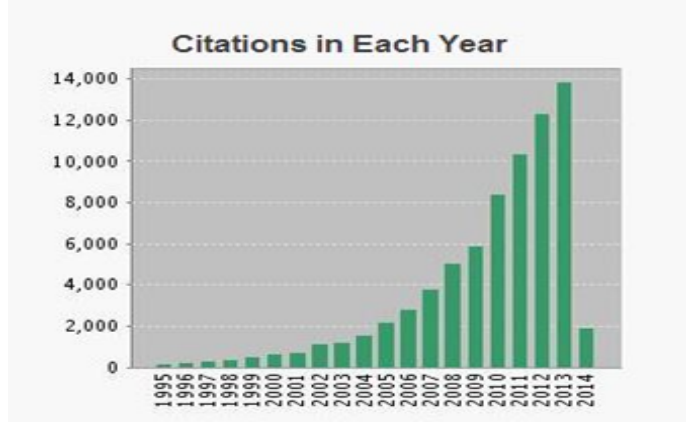


Figure 1.1: *Statistics of citations per year for the search string “transparent and conducting thin film films” upto Feb 2014 (from Web of Science).*

Where ρ is the resistivity, R is the resistance (in Ω), L is the length of the material (in cm) and A is the area of the film (in cm^2). The SI unit of the resistivity is Ωcm . The band gap of these films is ~ 3 eV (energy corresponding to wavelength 413.3nm calculated by the formula $E = hc/\lambda$), which makes them more than 80% transparent to wavelengths greater than 400 nm in thin film form. This combination of optical transparency and electric conductivity cannot be achieved in intrinsic stoichiometric oxides. So the oxides with non-stoichiometric compositions or oxides with appropriate doping are produced. The important TCO semiconductors are impurity-doped ZnO , I_2O_3 , SnO_2 and CdO , as well as the ternary compounds Zn_2SnO_4 , $ZnSnO_3$, $Zn_2In_2O_5$, Zn_3InO_6 , In_2SnO_4 , $CdSnO_3$ and multi-component oxides consisting of combinations of ZnO , In_2O_3 and SnO_2 .

The most popular TCOs are tin-doped indium oxide (ITO), fluorine doped tin oxide (FTO), and aluminum-doped zinc oxide (AZO). However, ITO films are most commonly used in electronics. This is due to the extraordinary combination of optical and electrical properties. ITO has intrinsic band gap of 3.7eV (energy corresponding to wavelength 335nm), electrical resistivity near $2 \times 10^{-4} \Omega cm$ and optical transparency greater than 80% [2].

2) Organic – They are prepared from carbon based compounds such as graphene, reduced graphene oxide (RGO), carbon nanotubes (CNT), polymers and composites of these. These TCFs can be produced using various methods due to which they show a wide range of conductivity and transparency. Using liquid-liquid assembly, hydrophobic films consisting of multilayer graphene platelets have been prepared which gives a sheet resistance of $100 \Omega/sq$. Sheet resistance is a special case of resistivity for a uniform sheet thickness and defined by

$$R_s = \frac{\rho}{t}$$

where ρ is the resistivity (in Ωcm), R_s is the sheet resistance and t is the thickness of the sheet (in cm). When resistivity is divided by the sheet thickness ($1/cm$), the units are $\Omega.cm.(cm/cm).1/cm = \Omega$. The term cm/cm cancels, but represented as special "square (sq)" which yields an answer in Ω/sq . The advantage with this unit is that, sheet resistance can be distinguished from bulk resistance by having the SI unit Ω/sq instead of just Ω . These films also had an optical transmittance of 70%

at 500 nm[3]. For the films prepared from RGO, transparency as large as 90% and sheet resistance as low as $100\Omega/sq$ can be achieved[4]. The films made from CNT and composites of CNTs are >80% transparent to visible light, as well as being transparent to IR light in the $2 - 5\mu m$ wavelength region having sheet resistance $100\Omega/sq$ [5].

3) Metallic films – TCFs can also be prepared from metallic grids and nanowires networks. The most commonly used metals for this purpose are silver, gold and copper. It has been reported that films made from silver nanowire networks show sheet resistance of $175\Omega/sq$ and transparency of 75% [6]. Also gold nanowires has been used for making flexible transparent conducting material[7]. The gold nanowires have also been used to prepare thin films giving sheet resistance $\sim 1100k\Omega/sq$ and transparency 90-97% [8].

1.1.1 Applications of TCFs

Due to the unique combination of conductivity and transparency, these TCFs have a lot of applications. Few of these applications are discussed below:

- Electromagnetic radiation interference (EMI) shielding - TCO coatings may be used as shielding to decrease EMI. This may be to either to keep radiation from escaping an enclosure or to avoid entering an enclosure to prevent external radiation sources from interfering with electronic devices within. One example is the window of domestic microwave ovens, which uses these type of coatings to reduce microwave leakage.

- Energy efficient coating – These conducting coating can be used for energy conserving purposes. For example they can be made infra-red (IR) reflecting in addition to being transparent and can be coated on the glass windows of air conditioned rooms. This leads to the good light transmission in the visible range, while minimizing heat transmission. The feature can be used to minimize air conditioning costs in the summer, and heating costs in the winter.

- Liquid crystal displays - In liquid crystal displays (LCDs), both electrodes need to be transparent and conducting, in order to allow backlighting to pass through the liquid crystal film while applying voltage to the various pixels. Generally these electrodes are in the form of a pattern of lines, with the alignment of the lines on the two electrodes perpendicular to each other. This allows addressing individual pixels by applying a voltage to the two lines which intersect at a given pixel.

- Flexible displays – As the name suggests flexible display is a display which is flexible in nature. Some organic TCFs which are flexible are being explored to be incorporated in these kinds of displays.

- Touch screens - These TCFs can be used in touchscreen devices like smart phones, navigation systems, digital cameras etc. The touchscreen panel consists of two thin, transparent, electrically resistive layers with a thin space between them. When the film surface is pressed with a finger or stylus, it comes into contact with the electrode film of the plate in the lower portion and starts the flow of an electric current. The change in voltage is then recognized, detecting the touch position.

- Organic light emitting diodes (OLED) - An OLED is a light emitting diode in which the electroluminescent layer is a film of organic compound, which emits light

in response to an electric current. This layer is situated between two electrodes, at least one of which is transparent. The transparent electrode is made from the TCO films.

- Solar cells - Most solar cells use TCO films as a transparent electrode. They serve the purpose of being conducting and transparent, along with that they are electronically compatibility with adjacent layers in the cell and stable under environmental conditions.

1.2 Need For the Replacement of TCOs

TCOs are the most commonly used transparent conducting material and in particular ITO. Although ITO serves the purpose of being extremely conductive, as well as nearly transparent to visible light for many applications, there are several disadvantages associated with it. These are given below

- Indium, which is present in ITO, is very expensive, rare and toxic.
- Equipment and techniques used for synthesizing ITO films are quite expensive.
- ITO has limited transparency and films made from it are fragile in nature. So these cannot be used in flexible displays.

Due to the above problems related to ITO films, other alternatives are being explored for the replacement. The best candidate for this purpose is organic thin film which was discussed in section 1.1. The advantages of organic thin films are

- Conductivity and transparency can be made comparable to the traditional TCOs.
- The materials used for making these films are inexpensive as well as non-toxic.
- These thin films have high elastic modulus and tensile strength making them suitable for flexible electronics.

Graphene is a very good material for producing organic TCFs with desired properties. However, the methods involved for synthesizing it, are quite complex and expensive. Also large scale production is a challenge. A simple method for producing graphene, is to synthesize GO and then reduce it. The same method is followed in this project for preparing organic thin films. Properties of graphene and GO are discussed in sections 1.3 and 1.4. Different approaches used for synthesizing GO and the advantages of the procedure followed in this project are also described in later sections.

Extremely thin films made from metallic grids and nanowires can also be a potential substitute for ITO. As discussed in section 1.1, these films also have comparable properties to that of ITO. In this project, metallic films were also synthesized using gold nanowires. Later a hybrid film of GO/gold nanowires was prepared.

1.3 Graphene

Graphene has recently emerged as a material having amazing properties and numerous applications. It was extracted from bulk graphite in 2004 by Andre Geim and Konstantin Novoselov from University of Manchester[8]. They used a very simple method in which they used scotch tape to remove the single layer of graphene from

the graphite. Basically, it is a 2D structure of single layer of carbon atoms as shown in fig. 1.2. The carbon atoms are arranged in a honey-comb lattice structure or hexagonal pattern and all of them are sp^2 hybridized.

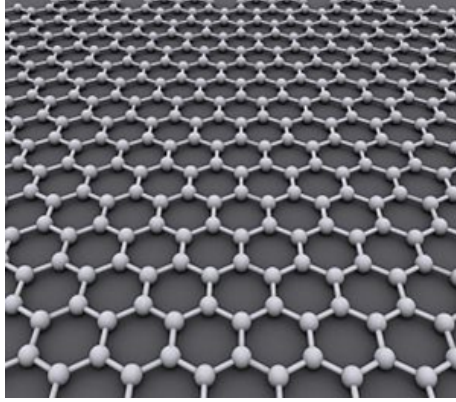


Figure 1.2: *Hexagonal arrangement of carbon atoms in graphene (from Wikipedia).*

Graphene has lots of unique and interesting properties as discussed below:

1. Morphology and structure – It is the thinnest material known till now. Single layer of graphene is ~ 0.4 nm thick. In the hexagonal structure, the carbon atoms are attached to each other by σ -bonds. Each carbon atom has π -electrons because of the sp^2 hybridization and they contribute to the conduction of graphene. Every gram of graphene has a surface area of $\sim 3000m^2$ which is the largest among all the materials.

2. Mechanical property - Because of strong covalent bond between the atoms, it is world's strongest material. The mechanical stiffness of graphene is 1,050 GPa[10]. It is nearly 100 times stronger than a hypothetical film of steel having same thickness but it is six times lighter.

3. Electronic property – The continuous π -electron network makes graphene an extremely good conductor of electricity. The resistivity of the single layer graphene sheet is of the order $10^{-6}\Omega cm$. The other carbon forms such as graphite and carbon nanotubes are also conducting having resistivity of the order $10^{-3} - 10^{-4}\Omega cm$ [11]. However diamond is an insulator and has very high resistivity of $\sim 10^{10}\Omega cm$.

Graphene is a zero band-gap semiconductor. A band gap is the gap between the energy of an electron when it is bound to an atom or valence band, and the conduction band, where it is free to move around. In graphene the valence band and the conduction meet at the Dirac point as shown in fig. 1.3(c). The energy-momentum relation or the dispersion relation is linear for low energies near the six corners of the two-dimensional hexagonal Brillouin zone. The relation is given by

$$E = \frac{h\nu_F}{2\pi} \sqrt{k_x^2 + k_y^2}$$

Where h is the Plank's constant, ν_F is the Fermi velocity, k_x and k_y are the x and y components of the wavevector. This leads to zero effective mass for electrons and holes, making them behave like relativistic particles described by the Dirac equation

for spin-1/2 particles. It has been reported that the band-gap of graphene can be tuned by doping it for desired applications.

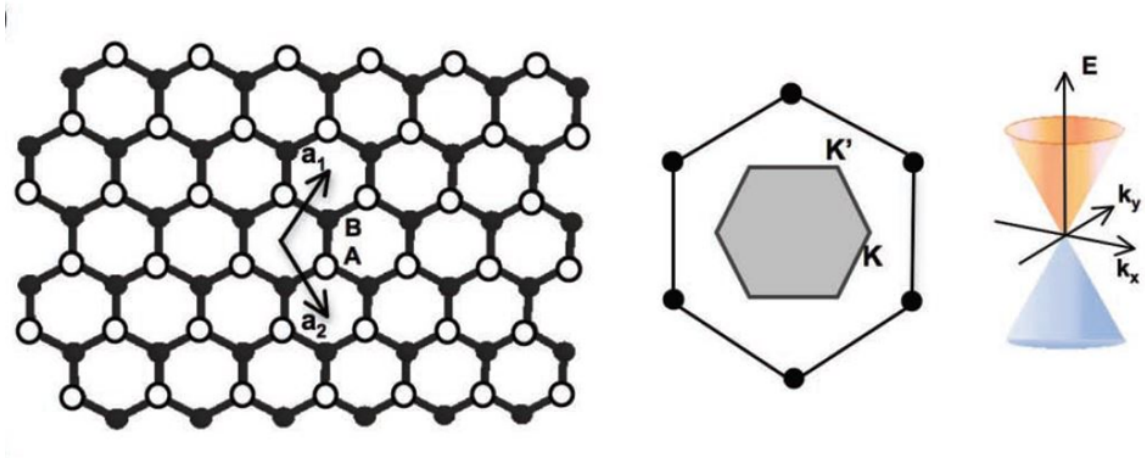


Figure 1.3: (a) Schematics of the crystal structure (b) Brillouin zone (c) dispersion spectrum of graphene[12].

At room temperature, it has high electron mobility with reported values in excess of $15000\text{cm}^2\text{V}^{-1}\text{s}^{-1}$. It is said that graphene electrons act very much like photons in their mobility due to their lack of mass.

4. Optical Property – Only one atom thick layer of graphene can absorb 2.3% of white light. Due to the unique electronic structure in which conduction and valence bands meet at the Dirac point, the optical conductance of pristine monolayer graphene is frequency-independent. As a consequence, the optical transmittance of pristine graphene is also frequency-independent.

5. Thermal Property – Graphene is also highly conducting to heat. The thermal conductivity of graphene measured at room temperature is in the range $2000 - 4000\text{Wm}^{-1}\text{K}^{-1}$. This value is much higher than the value observed in all the other carbon structures as carbon nanotubes, graphite and diamond.

1.4 Graphene Oxide (GO)

Individual sheets of graphene attached with oxygen containing functional groups are called GO. Single layer of GO is $1.1 \pm 0.2\text{nm}$ thick. It was first prepared in 1859 by oxidizing the graphite. Later various methods for synthesizing GO were developed, which will be discussed in the next section. In GO, the oxidation of graphene sheet is not uniform throughout. Ratio of carbon to oxygen is not fixed, it depends on the method by which GO is prepared. There are two regions in it: non-oxidized and oxidized. Because of incomplete oxidation, some carbon atoms

retain the sp^2 hybridization and form the non-oxidized part. Oxidized region contains sp^3 hybridized carbon atoms to which oxygen containing functional groups such as hydroxyl, ketones, epoxy, carboxyl and carbonyl are attached. The epoxy functional groups are present along the basal plane of sheets and hydroxyl and carboxyl groups at the edges. The structure of GO is shown in fig 1.4.

There are various interesting properties of GO as discussed below:

1. Reduction to Graphene – The most important property of GO is that, it can be converted to RGO which shows properties close to graphene. In terms of electrical conductivity, GO is an insulator because of the disruption in the sp^2 network. As it is reduced, the network is restored and GO becomes conducting. The RGO is prepared by carrying out reduction of GO. The reduction process involves removal of the oxygen containing functional groups. There are several ways by which reduction is carried out, each giving different results.

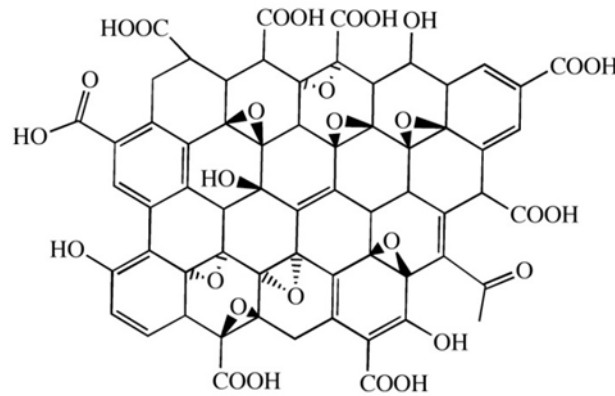


Figure 1.4: Structure for GO. Adapted from C. E. Hamilton, PhD Thesis, Rice University (2009).

2. Solubility – GO is amphiphilic in nature in contrast to graphene which is highly hydrophobic [13]. Due to the presence of various oxygen containing functional groups, it is easily dispersible in water and organic solvents.

3. Chemical activity - GO exhibits enhanced chemical activity due to the functional groups attached to it. These serve as sites for chemical modification or fictionalization. Fictionalization of GO can change its properties, resulting in chemically modified graphene that could then have a lot of applications.

4. Band gap varies depending on the oxidation level. energy gap in GO can be tuned through controlled reduction processes.

1.4.1 Synthesis of GO

There are two approaches by which GO is synthesized

1) Top down approach – This approach uses graphite as the precursor. Upon oxidation using strong oxidizers, graphite is converted to graphite oxide. Monolayer

or few layers of GO is obtained by the exfoliation of graphite oxide. In 1859, GO was synthesized by Brodie for the first time. He added a portion of potassium chlorate to slurry of graphite in fuming nitric acid [14]. Later, Staudenmaier improved this protocol in 1898 by using concentrated sulfuric acid as well as fuming nitric acid and adding the chlorate in multiple aliquots over the course of the reaction [15]. In 1958, Hummers reported the method most commonly used today. This method uses a mixture of sulfuric acid, sodium nitrate and potassium permanganate for the oxidation of graphite[16]. Recently some modifications has been reported in the Hummer's method for the improved synthesis of GO[16].

But there are several disadvantages associated with this approach. These are

- These methods are non-environment friendly because they use strong oxidizers which are toxic in nature.

- Multi steps involved in the synthesis.
- Very small flake are produced.
- Thickness of the flakes cannot be controlled.

2) Bottom up approach – It uses sugars as the sole reagent. Sugar molecules act as the precursor, which then polymerize to form the 2D GO films. Hydrothermal synthesis uses this bottom up approach[18].

The advantages with this method are

- Synthesis is environment friendly.
- The method is very simple and facile.
- Flakes produced have large area.
- Thickness can be controlled by controlling the reaction parameters.

In this project, the hydrothermal method was used for the synthesis, the detailed procedure of which is discussed in chapter 2. Using this method, large area sheets (upto $1.7mm^2$) were synthesized. As the sugar solution is heated, the sugar molecules polymerize and water molecules are released. Changing the reaction conditions gives films of different thickness. As the time of reaction or the temperature or the concentration of sugar solution is increased, more of the sugar molecules polymerize and multilayered films are produced. This mechanism of formation of GO is described in fig. 1.5.

Using the above method, different films were synthesized. They were found to be upto 90% transparent in the visible region. Also to make them conducting, reduction process was carried out and detailed procedure of which will be discussed in chapter 2. The characterization of these films and the results for transparency and conductivity will be discussed in chapter 3.

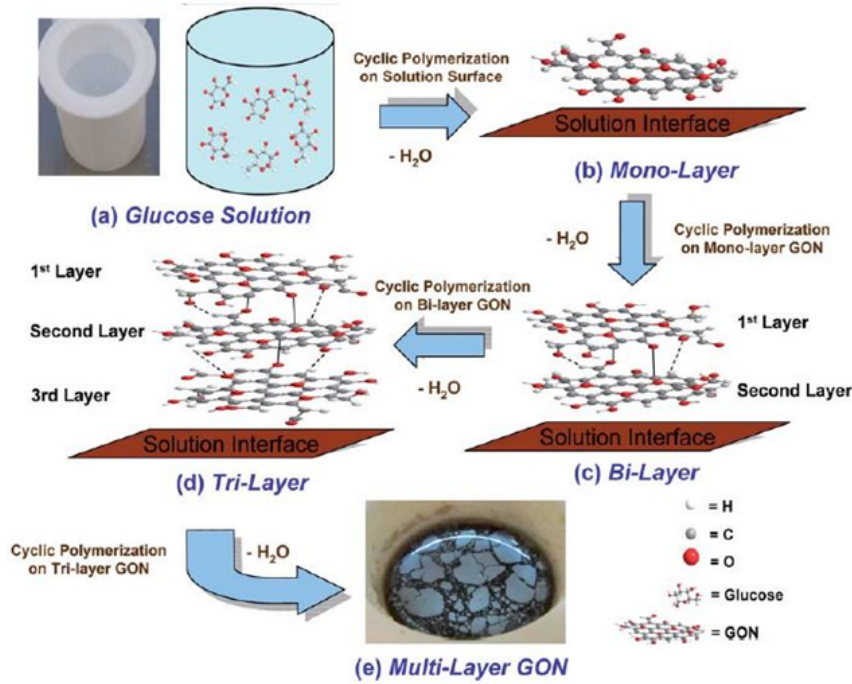


Figure 1.5: Schematic illustration of the bottom-up synthesis mechanism of GO. (a) sugar molecules undergo cyclic polymerization (b) monolayer of GO floats on solution (c) the second layer GO may be grown underneath the first GO layer forming a bi-layer GO (d) subsequently, tri-layer (e) and multilayer GO can be produced [18].

1.4.2 Reduction of GO

The main purpose for the reduction of GO is to achieve better conductivity. As synthesized GO is insulating in nature (sheet resistance $> 10^9 \Omega/sq$). Reason behind the high value of resistance for GO is the disturbance in the conjugation of π -electrons. In graphene all the carbon atoms are sp^2 hybridized leading to delocalization of π -electrons throughout the graphene film and hence very good conductivity. However in GO, carbon atoms to which oxygen containing functional groups are attached becomes sp^3 hybridized. This leads to the disruption in the delocalization in the π -electrons and that is why GO has high resistance. By the removal of these functional groups, π -network can be restored and resistance of GO can be significantly decreased. There are several methods by which reduction of GO can be done. These are given below

- Thermal reduction - High temperature annealing ($1100^\circ C$) of GO leads to the removal of most of the functional groups making GO conducting. By this method sheet resistance as low as $10^2 \Omega/sq$ can be achieved [19].
- Photoreduction - This includes microwave and UV irradiation of GO leading to the resistance in the range $100 \Omega/sq - 10 M\Omega/sq$ [20].
- Chemical reduction - Reducing agents such as sodium borohydride ($NaBH_4$), hydrazine (N_2H_4), hydroiodic acid (HI) are also used for the reduction of GO.

This approach alone does not give low resistance because of selective removal of functional groups. This method produces GO films with resistance $>100M\Omega/sq$ [21].

- Combination of chemical and thermal reduction - This method includes the chemical reduction and low temperature annealing ($400^{\circ}C$) and results in the intermediate value of resistance for GO films in the range $1k\Omega/sq - 0.5M\Omega/sq$ [19].

In the project last method was used for the reduction of GO, the detailed procedure of which will be given in chapter 2. The results obtained from the reduction of GO films will be discussed in detail in chapter 3.

1.5 Gold Nanowires (AuNWs)

Gold is one of the least reactive chemical elements. The atomic number of gold is 79 and has electronic configuration $[Xe]4f^{14}5d^{10}6s^1$. It is a transition metal and group 11 element. It is dense, ductile and malleable metal with bright yellow colour and luster. Some of the bulk properties of gold are listed in table 1.1.

Properties	Values
Atomic mass	$196.9655gmol^{-1}$
Density	$19.30gcm^{-3}$
Electrical resistivity	$2.21 \times 10^{-6}\Omega cm$
Thermal conductivity	$318Wm^{-1}K^{-1}$
Young's Modulus	$79GPa$
Oxidation states	5, 4, 3, 2, 1, -1
Melting point	$1064.18^{\circ}C$
Boiling point	$2970^{\circ}C$
Lattice structure	FCC

Table 1.1: *Bulk properties of gold*

Gold can be converted into various nanostructures having different morphologies. Nanoparticles, nanorods, nanowires, nanostars are some of the common nanostructures of gold. Depending upon the size and morphology, the gold shows different properties.

AuNWs are 1-D nanostructures of gold. They have large aspect ratio (length to diameter ratio) having length in micrometers and diameter of few nanometers. Due to the large anisotropy of AuNWs and their ability to self-assemble they can become important building blocks for the linkage of nanoscale electronics and molecular devices[22],[23]. They can also be used to make thin films which are transparent and conducting[8].

1.5.1 Optical Properties of Au NWs

Optical properties of metals are determined by the dielectric constants. For the noble metals (Ag, Au and Cu) the dielectric constants are a function of the incident

electromagnetic (EM) wavelengths, and hence these metals display interesting properties. In 1908 Gustav Mie theoretically described the optical properties of the metal particles with sizes extremely less than EM wavelengths[24]. He stated that there is a size independent resonant absorption of the incident energy at a specific (material dependent) wavelength. In 1912, Richard Gans extended this theory for anisotropic small metal particles[25]. He obtained a size dependent behavior of a resonant absorption of the incident energy. Later on Paul Drude described the properties of conduction electrons in metals in 1900[26]. He stated that these electrons undergo collective oscillations in response to incident EM waves, which are characterized by the plasma frequency (metal specific). A quantum of such specific oscillating electrons is termed as plasmon, and they determine the optical behavior of these metals. In the case of metal nanoparticles, the surface area to volume ratio is very high and the contribution to their optical properties comes from surface plasmons. When the natural frequency of the surface plasmons matches with that of incident EM waves resonant absorption occurs, termed as surface plasmon resonance (SPR).

Au NWs are 1D anisotropic nano structures of gold. Thus the optical properties of Au NWs can be deduced from Gans theory. For anisotropic nanostructures there are two distinct modes of electron oscillations i.e. plasmons. When the incident EM waves is polarised perpendicular to the long axis of the nanowires, the mode of oscillation is termed as transverse surface plasmons (TSP). In the case of Au, the TSP resonance occurs at incident wavelength between 520-530 nm (green). Since the green wavelengths are absorbed, Au NWs typically appear red/pink colour (fig. 1.6). The other mode of the oscillation is the longitudinal surface plasmon mode (LSP), for incident polarization along the long axis of the nanowires. LSP resonances typically occur in the IR region and hence do not show in the visible range of the EM spectra.



Figure 1.6: Solution of gold nanowires showing the red/pink colour.

1.5.2 Synthesis of Au NWs

There are several methods by which AuNWs with desired shapes can be produced. Particle assembly[27], surfactant mediation[28], template assistance[29] or physical deposition[30] are some of the common methods. However, these methods have several disadvantages. Lengthy reaction time, high temperature treatment, complicated steps, poor morphology of the produced nanowires are some of these problems.

In this project, a wet chemical method was adopted for the synthesis of ultrathin Au NWs[31]. The detailed procedure of the synthesis will be discussed in chapter 2. This is a one-step method, in which the reaction takes place at room temperature. The wires produced have capping agent on them which prevents them from aggregating as shown in fig.1.7. They are very uniform and have good morphology.

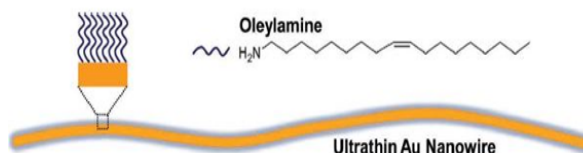


Figure 1.7: *Ultrathin gold nanowires with capping agent*[8].

These nanowires have been used for the synthesis of TCFs with good transparency[8]. In this project, nanowires were used to prepare thin films which were transparent (>80%) in the visible region. Also a hybrid film of GO/AuNWs was synthesized. The characterization of these films and other results will be discussed in chapter 3 in more detail.

1.6 Summary

In this chapter, the types, properties and applications of TCFs in different fields were discussed in detail. ITO is the most commonly used TCFs at present. However, there is a need for replacement for ITO which was discussed in the subsequent section. Organic and metallic thin films are good candidates for this purpose. This project was focused to prepare TCFs using RGO, AuNWs and a composite of these two which can possibly be used as the alternatives for ITO. The properties and synthesis methods for these materials were discussed in the last sections.

1.7 Bibliography

1. H. Kim, J. S. Horwitz, G. P. Kushto, Z. H. Kafafi, and D. B. Chrisey, “Indium tin oxide thin films grown on flexible plastic substrates by pulsed-laser deposition for organic light-emitting diodes”, *Appl. Phys. Lett.*, Vol. 79, No. 3, July **2001**.
2. C. Guillén and J. Herrero, “Critical review TCO / metal / TCO structures for energy and flexible electronics,” *Thin Solid Films*, vol. 520, no. 1, pp. 1–17, **2011**.
3. S. Biswas and L. T. Drzal, “A Novel Approach to Create a Highly Ordered Monolayer Film of Graphene Nanosheets at the Liquid–Liquid Interface,” *Nano Lett.*, vol. 9, no. 1, pp. 167–172, Dec. **2008**.
4. H. A. Becerril, J. Mao, Z. Liu, R. M. Stoltenberg, Z. Bao, and Y. Chen, “Evaluation of Solution-Processed Reduced Graphene Oxide Films as Transparent Conductors,” *ACS Nano*, vol. 2, no. 3, pp. 463–470, Feb. **2008**.

5. N. Saran, K. Parikh, D.-S. Suh, E. Muñoz, H. Kolla, and S. K. Manohar, "Fabrication and Characterization of Thin Films of Single-Walled Carbon Nanotube Bundles on Flexible Plastic Substrates," *J. Am. Chem. Soc.*, vol. 126, no. 14, pp. 4462–4463, Mar. **2004**.
6. C. Liu and X. Yu, "Silver nanowire-based transparent, flexible, and conductive thin film," *Nanoscale Res. Lett.*, vol. 6, no. 1, p. 75, **2011**.
7. D. Langley, C. Celle, D. Bellet, and J. Simonato, "Flexible transparent conductive materials based on silver nanowire networks: a review," *Nanotechnology*, vol. 45, **2001**.
8. Chen, Yi Ouyang, Zi Gu, Min Cheng, Wenlong, "Mechanically Strong, Optically Transparent, Giant Metal Superlattice Nanomembranes From Ultrathin Gold Nanowires," *Adv. Mater.*, vol. 25, pp. 80-85, **2013**.
9. A. A. F. K.S. Novoselov, A.K. Geim, S.V. Morozov, D. Jiang, Y. Zhang, S.V. Dubonos, I.V. Grigorieva, "Electric Field Effect in Atomically Thin Carbon Film," *Science*, vol. 22, pp. 2–6, **2004**.
10. F. Liu, P. Ming, and J. Li, "Ab initio calculation of ideal strength and phonon instability of graphene under tension," *Phys. Rev. B*, vol. 76, no. 6, p. 064120, **2007**.
11. Bernardo Marinho, Marcos Ghislandi, Evgeniy Tkalya, Cor E. Koning, Gijbertus de With, "Electrical conductivity of compacts of graphene, multi-wall carbon nanotubes, carbon black, and graphite powder", *Powder Technology*, vol. 221, pp. 351–358, **2012**.
12. B. Y. Zhu, S. Murali, W. Cai, X. Li, J. W. Suk, J. R. Potts, and R. S. Ruoff, "Graphene and Graphene Oxide: Synthesis, Properties, and Applications," *Adv. Mater.*, pp. 3906–3924, **2010**.
13. O. Leenaerts, B. Partoens, and F. M. Peeters, "Water on graphene: Hydrophobicity and dipole moment using density functional theory," *Phys. Rev. B*, vol. 79, no. 23, pp. 235440, **2009**.
14. Brodie, B. C. On the Atomic Weight of Graphite, *Philos. Trans. R. Soc. London*, vol. 14, pp. 249–259, **1859**.
15. Staudenmaier, L. Verfahren zur Darstellung der Graphitsäure., *Ber. Dtsch. Chem. Ges.*, vol. 31, pp. 1481–1487, **1898**.
16. W. S. Hummers and R. E. Offeman, "Preparation of Graphitic Oxide," *J. Am. Chem. Soc.*, vol. 80, no. 6, p. 1339, Mar. **1958**.
17. D. C. Marcano, D. V. Kosynkin, J. M. Berlin, A. Sinitskii, Z. Sun, A. Slesarev, L. B. Alemany, W. Lu, and J. M. Tour, "Improved Synthesis of Graphene Oxide," *ACS Nano*, vol. 4, no. 8, **2010**.
18. Libin Tang, Xueming Li, Rongbin Ji, Kar Seng Teng, Guoan Tai, Jing Ye, Changsong Wei and Shu Ping Lau, "Bottom-up synthesis of large-area graphene oxide nanosheets," *J. Mater. Chem.*, vol. 22, pp. 5676–5683, **2012**.

19. H. A. Becerril, J. Mao, Z. Liu, R. M. Stoltenberg, Z. Bao, and Y. Chen, "Evaluation of Solution-Processed Reduced Graphene Oxide Films as Transparent Conductors," *ACS Nano*, vol. 2, no. 3, pp. 463–470, **2008**.
20. Zhang Yong-lai, Guo Li, Xia Hong, Chen Qi-dai, Feng Jing, Sun Hong-bo, "Photoreduction of Graphene Oxides : Methods , Properties , and Applications", *Adv. Optical Mater.*, **2013**.
21. Mao Shun, Pu Haihui, Chen Junhong, "Graphene oxide and its reduction : modeling and experimental progress", *RSC Adv.*, vol. 2, pp. 2643-2662, **2012**.
22. J. Huang, R. Fan, S. Connor, and P. Yang, "One-step patterning of aligned nanowire arrays by programmed dip coating.," *Angew. Chem. Int. Ed. Engl.*, vol. 46, no. 14, pp. 2414–7, Jan. **2007**.
23. T. Wang, X. Hu, J. Wang, and S. Dong, "Surface-enhanced Raman scattering from surfactant-free 3D gold nanowire networks substrates.," *Talanta*, vol. 75, no. 2, pp. 455–60, Apr. **2008**.
24. G. Mie, *Ann. Phys.*, vol. 330, pp. 377–445, **1908**.
25. R. Gans, *Ann. Phys.*, vol. 342, pp. 881–900, **1912**.
26. N. W. Aschroft and N. D. Mermin, "Chapter 1," in *Solid State Physics*, 1st ed., Orlando, FL, USA: Harcourt College Publishers, pp. 1–28, 1976.
27. L. Pei, K. Mori, and M. Adachi, "Formation process of two-dimensional networked gold nanowires by citrate reduction of AuCl₄⁻ and the shape stabilization.," *Langmuir*, vol. 20, no. 18, pp. 7837–43, Aug. **2004**.
28. X. Liu, N. Wu, B. H. Wunsch, R. J. Barsotti, and F. Stellacci, "Shape-controlled growth of micrometer-sized gold crystals by a slow reduction method.," *Small*, vol. 2, no. 8–9, pp. 1046–50, Aug. **2006**.
29. H. Bai, K. Xu, Y. Xu, and H. Matsui, "Fabrication of Au nanowires of uniform length and diameter using a monodisperse and rigid biomolecular template: collagen-like triple helix.," *Angew. Chem. Int. Ed. Engl.*, vol. 46, no. 18, pp. 3319–22, Jan. **2007**.
30. C. E. Cross, J. C. Hemminger, and R. M. Penner, "Physical vapor deposition of one-dimensional nanoparticle arrays on graphite: seeding the electrodeposition of gold nanowires.," *Langmuir*, vol. 23, no. 20, pp. 10372–9, Sep. **2007**.
31. H. Feng, Y. Yang, Y. You, G. Li, J. Guo, and T. Yu, "Simple and rapid synthesis of ultrathin gold nanowires , their self-assembly and application in surface-enhanced Raman scattering ," *Chem. Comm.*, pp. 1984–1986, **2009**.

Chapter 2

Experimental Methods and Techniques

In this chapter, the methods used for synthesis and reduction of graphene oxide (GO), synthesis of gold nanowires (Au NWs) and graphene oxide/gold nanowires (GO/Au NWs) composite are discussed. Later, the working principle of the techniques used for characterization like UV-Vis Spectroscopy (UV), Scanning Electron Microscopy (SEM), Atomic Force Microscopy (AFM), Raman Spectroscopy, Fourier Transform Infrared Spectroscopy (FTIR) and Four Probe are described.

2.1 Synthesis Methods

2.1.1 Hydrothermal Synthesis of GO

In this project, GO was prepared using hydrothermal method [1]. Following the bottom up approach, synthesis was carried out using sugars as the sole reagent. The sugars used were glucose ($C_6H_{12}O_6$), lactose ($C_{12}H_{22}O_{11}$), sucrose ($C_{12}H_{22}O_{11}$) and galactose ($C_6H_{12}O_6$). Glucose was purchased from Sigma Aldrich Inc., sucrose and lactose were purchased from Merck and galactose was purchased from Sd. fine Chem limited. Initially glucose was used for the synthesis. In a particular reaction, 100 mL of 0.65 M glucose solution in distilled water was taken. 90 mL of the solution was poured in a 100 mL Teflon container, which was then kept in an autoclave. The temperature was set to 190°C and the solution was kept for 9 hours. After the completion of the reaction, the solution was left to cool down to room temperature. Films were formed because of the cyclic polymerization of sugar on the surface of the solution. They were then deposited on glass and silicon substrate and then dried for further characterization.

Different syntheses were carried out by varying the reaction parameters. The concentrations used were 0.325M and 0.65M, temperature was varied between 165 – 200°C and the time variation ranged from 3 hours to 10 hours. Later, other sugars such as lactose, sucrose and galactose were used. In this case, by keeping the temperature and concentration of the sugar solution constant, the time for the reaction was varied.

2.1.2 Reduction of GO

GO can be reduced to give graphene, also known as reduced graphene oxide (RGO). The main purpose of reduction is the removal of oxygen containing functional groups and restoring the sp^2 network. As the network is reconstructed, the π -electrons contribute to conduction of GO. As discussed in chapter 1, there are various reduction methods by which RGO is synthesized and each method produces RGO with different properties.

Here, the combination of chemical reduction and thermal annealing was used for the reduction of GO [2]. Hydrazine monohydrate ($N_2H_4.H_2O$) purchased from Sigma Aldrich vapor was used as the reducing agent for chemical reduction. GO films deposited on the glass substrate were kept in a beaker inside a larger beaker. 1 mL of hydrazine monohydrate was added to the larger beaker, covered with a glass lid, sealed with scotch tape and kept on the hot plate at $40^\circ C$ for 18 hours. After the completion of reaction, the film was rinsed with distilled water and dried both under nitrogen flow and by heating at $80^\circ C$ in vacuum.

Chemically reduced GO film deposited on glass substrate, was then heated at a rate of $13.3^\circ C/min$, held at $400^\circ C$ for 3 hours and allowed to cool down to room temperature in 1 hour. All the heating process was carried out under the continuous flow of argon gas in a tube furnace.

2.1.3 Synthesis of Au NWs

Au NWs were synthesized using a very simple and one-step wet chemical method [3]. Gold chloride ($AuCl_3$), oleylamine (OA) ($C_{18}H_{37}N$) and triisopropylsilane (TIPS) ($C_9H_{22}Si$) was purchased from Sigma Aldrich and hexane (C_6H_{14}) was purchased from Rankem. In a particular synthesis, $3mg$ of gold chloride was added to $2.5mL$ of hexane, followed by the addition of $100\mu L$ OA and $150\mu L$ TIPS which gave a yellow solution. This solution was left for 12 hours at room temperature without stirring. The colour of the solution gradually changed to dark red. As OA was mixed with gold chloride, a complex was formed between these two, forming a polymeric chain kind of structure. TIPS reduced $Au(III)$ to $Au(0)$ which produced OA capped nanowires. To remove the excess OA and TIPS, the final products were centrifuged, washed with ethanol and re dispersed in hexane.

2.1.4 Synthesis of GO/Au NWs Composite

GO/Au NWs composite was synthesized by a self-devised method as follows. In the first step, GO was synthesized following the procedure described in section 2.1.1. It was then deposited on silicon and glass substrates. The growth solution for Au NWs was prepared by mixing all the chemicals as described in the previous section. GO deposited on the substrate was put in this solution immediately and this system was kept at room temperature. After 12 hours, GO was removed and washed with ethanol and hexane to remove the extra capping agents. Washing was carried out by dipping the GO film deposited on the substrate in ethanol and hexane 2-3 times.

2.2 Characterization Techniques

2.2.1 UV-Vis Spectroscopy

This spectroscopic technique measures the absorption of a given sample (atoms, molecules or ions) in the UV and/or Vis region when electromagnetic radiation falls on it. Whenever the energy of incident radiation matches with that of any electronic transition of the sample, absorption takes place. This is observed in the form of a peak, when absorbance of the sample is plotted against the incident wavelength.

The absorbance is directly proportional to the path length and concentration of the absorbing species. This relation is also known as Beer-Lambert law and expressed as:

$$A = \log \frac{I}{I_0} = \epsilon bc$$

Where, I_0 is the intensity of incident radiation, I is intensity of transmitted radiation, ϵ is molar absorptivity, b is the path length of the sample and c is the concentration of absorbing species.

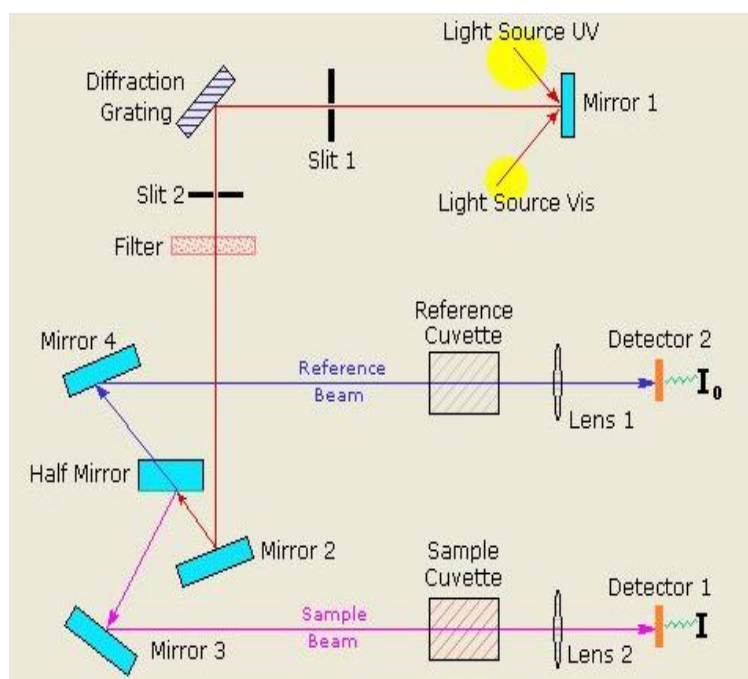


Figure 2.1: Schematic diagram of UV-Vis Spectrometer.

A schematic diagram of UV-Vis spectrophotometer is shown in Fig. 2.1 [4]. A beam of light from a visible and/or UV source falls on a mirror which is then reflected. The reflected beam is then separated into its component wavelengths after passing through a diffraction grating. Desired range of wavelength is selected from the filter and then focused on the half mirror. Each monochromatic wavelength is split into two equal intensity beams by the half mirror. One of the beams passes through the reference cuvette, containing only the solvent and the other beam passes through the sample cuvette which contains sample dissolved in the solvent. The intensities of these beams are recorded by the detectors and then compared.

In this project, Perkin Elmer Lambda 950 UV-Vis Spectrometer was used for the measurements. This equipment uses D_2 lamp as the source for UV light and tungsten lamp for visible light source. The absorption and transmission of solution as well as solid phase samples (thin films) were recorded.

2.2.2 Scanning Electron Microscope (SEM)

SEM is one of the most important characterization techniques in the field of nanoscience. It is extensively used in the morphological study of the samples. This is a type of microscope, which uses electrons instead of visible light for the high resolution imaging. Typically electrons are accelerated upto $\sim 30keV$ and resolution of $3 - 5nm$ can be achieved. Sometimes cold cathode is used for the emission of electrons under the application of high electric field. These types of SEMs are called Field Emission Scanning Electron Microscope (FESEM). The advantage with using electrons is that their wavelength can be tuned to a very small value and better resolution can be achieved.

The interaction between electrons and solid sample results into back scattering of electrons, production of Auger electrons, visible light, UV light, X-rays etc. depending upon the energy of electrons, type and thickness of sample. The beam of electrons becomes defocussed after interaction with solid and form a tear shape volume of beam interaction. SEM uses backscattered electron from the sample for imaging.

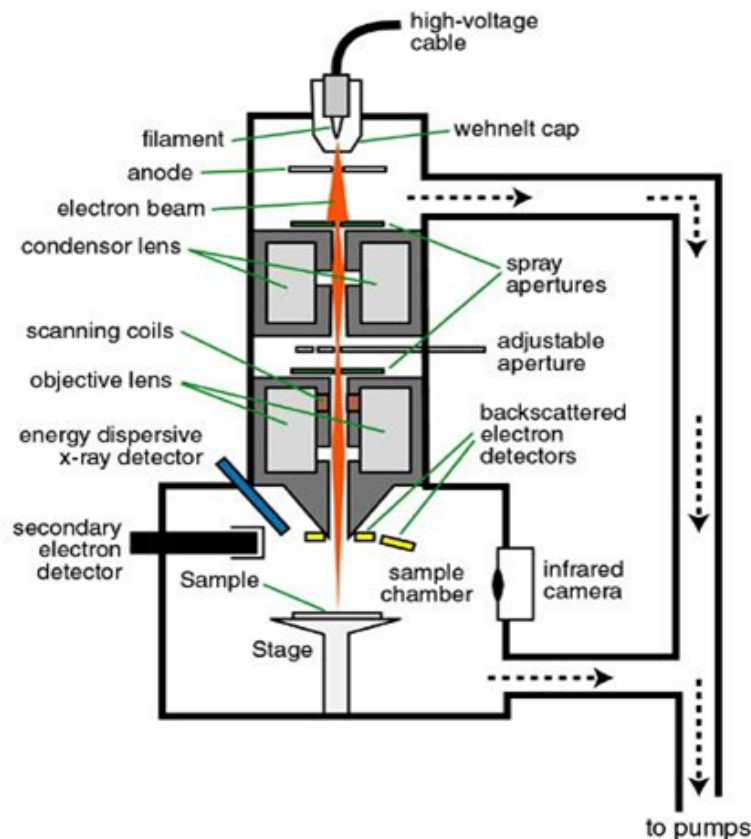


Figure 2.2: Schematic diagram of Field Emission Scanning electron microscope.

In fig 2.2 [5], the essential parts of FESEM are shown. The electron beam is produced by the filament and drawn away by the anode. The condenser lens controls the amount of current that passes down the rest of the column. This is accomplished by focusing the electron beam to variable degrees onto a lower aperture. The beam is again divergent after passing through the apertures below the condenser lens and must be refocused. The objective lens focuses the electron beam onto the sample and controls final size and position. Within it scanning coils are present, that allow the beam to be rastered across the sample. In the sample chamber, the beam falls on the sample kept on the stage. The microscope is held within a vacuum with the help of vacuum pump in order to properly focus the electrons on the sample.

In this project Carl Zeiss FESEM instrument was used for all the imaging. It has W/ ZrO Cathode which emits electron beam and accelerating voltage of $3 - 30keV$ was used. For imaging, the samples were drop casted on the silicon substrate and dried. For non-conducting samples, gold coating was done to make them conducting.

2.2.3 Atomic Force Microscope (AFM)

AFM is another technique for studying the morphology of the samples. The most significant feature of AFM is that it can be used to study non-conducting as well as conducting samples.

As shown in fig. 2.3(a) [6], AFM consists of a sharp tip on the end of a flexible cantilever which moves across a sample surface. The tips typically have an end radius of $2 - 20nm$, depending on tip type and the cantilever is $100\mu m$ long, $10\mu m$ wide and $1\mu m$ in height. As scanning takes place over the surface of sample, the force of interaction between the tip and the atoms leads to the deflection of tip. This deflection can be explained by taking the example of two atoms very close to each other. The interaction between the two atoms is described by Lennard-Jones potential given by the equation

$$V = \frac{A}{R^{12}}\hat{r} - \frac{B}{R^6}\hat{r}$$

Where V is the potential between two atoms, A and B are constants, R is the distance between the atoms and \hat{r} is the unit vector along the line joining the two atoms. When the separation R is very small, the first term dominates, and the potential is strongly positive. In contrast the second term predominates when the separation R increases in magnitude. Hence at very small distances repulsion between the atoms takes place and at larger distances the two atoms attract each other. The graph for Lennard-Jones potential is shown in figure 2.3(b).

A laser beam is focused on the back side of the cantilever, which is then reflected such that it is detected by the photodetector.

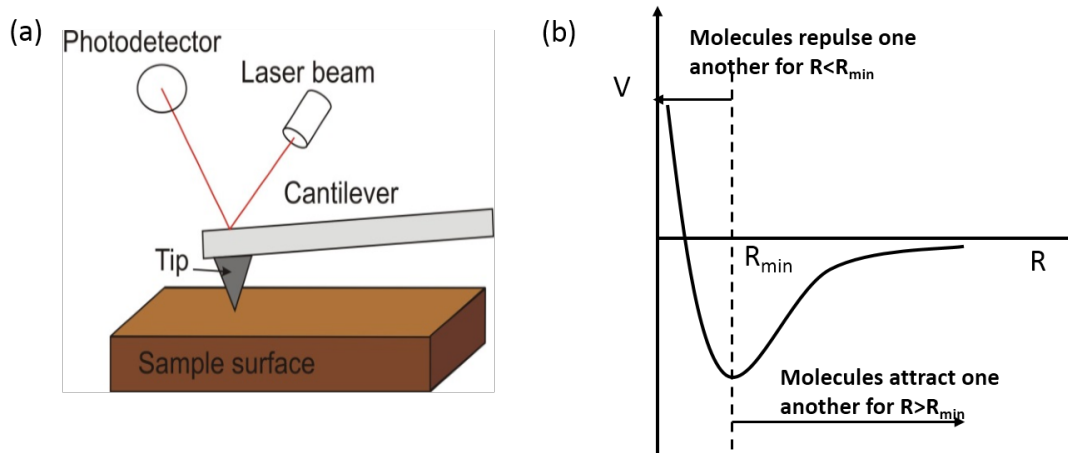


Figure 2.3: (a) Schematic of Atomic force microscope (b) Lennard-Jones potential.

There are three modes in which AFM can be operated.

- 1) Contact mode: The tip remains in contact with the sample surface.
- 2) Non-contact mode: In this mode, the tip moves at some small distance from the sample.
- 3) Tapping mode: It is a combination of contact and non-contact modes.

In this project, Nanosurf Easyscan Flex AFM was used for finding out the thickness of GO films. The samples were deposited on the silicon substrate and dried for the imaging. All the imaging was done in the tapping mode.

2.2.4 Fourier Transform Infrared Spectroscopy (FTIR)

FTIR is an important spectroscopic technique for the determination of types of bonds present in any compound. The principle behind infrared spectroscopy is the transition between vibrational energy levels of the molecules after interaction with the infrared (IR) light. The energy E_n of vibrations are given as

$$E_n = \left(n + \frac{1}{2}\right)h\nu_o$$

Where n is the quantum number for vibrational levels ($n = 1, 2, 3, \dots$), h is the Planck's constant and ν_o is the frequency of light. The transition occurs after absorption of photons following the selection rule $\Delta n = \pm 1$. Additionally, IR absorption takes place by any molecule only when it has a dipole moment.

FTIR spectrometer use Michelson interferometer for recording the spectra. The basic set-up of the spectrometer is shown in fig. 2.4 [7]. The light source sends all the source energy through the interferometer and onto the sample. In every scan, all source radiation gets to the sample. The light passes through a beam splitter, which sends the light in two directions at right angles. One beam goes to a stationary mirror then back to the beam splitter. The other goes to a moving mirror. The motion of the mirror makes the total path length variable versus that taken by the stationary-mirror beam. When the two meet up again at the beam splitter, they

recombine, but the difference in path lengths creates constructive and destructive interference.

The recombined beam passes through the sample. The sample absorbs all the different wavelengths characteristic of its spectrum, and this subtracts specific wavelengths from the interferogram. The detector now reports variation in energy versus time for all wavelengths simultaneously. Since all wavelengths are passing through the interferometer, the interferogram is a complex pattern. The absorption spectrum is obtained from the Fourier transform of the interferogram, which converts an intensity-vs.-time spectrum into an intensity-vs.-frequency spectrum.

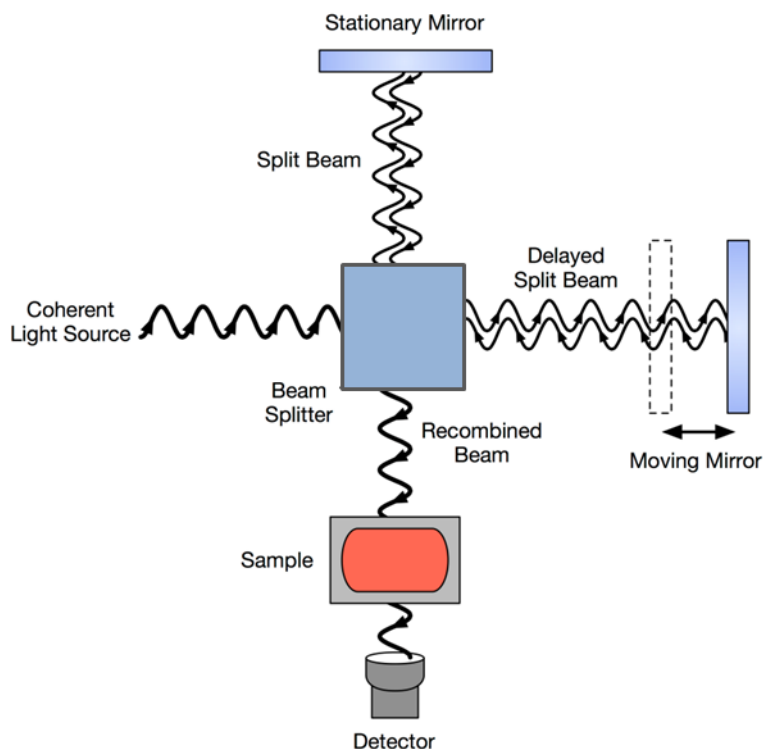


Figure 2.4: *Schematic diagram of FTIR set-up.*

In the project, Thermo Scientific Nicolet 6700 FTIR instrument was used for the determination of different type of functional groups present in GO. The FTIR spectra were obtained by mixing the sample with KBr powder and pellet was made out of it for the solid phase measurement.

2.2.5 Raman Spectroscopy

This is another technique used to observe vibrational, rotational, and other low-frequency modes in a system. When monochromatic light is directed on a molecule, the light can be scattered or absorbed. Most of the scattered light has same frequency as the incident light. This is known as Rayleigh scattering or elastic scattering. Raman spectroscopy depends upon the inelastic scattering (also known as Raman scattering) of light by the molecules. The scattered light can have either higher or lower energy compared to the incident light which depends upon the vibrational state of the molecule. If the energy of the scattered radiation is less then

it is called Stokes line and the radiation with more energy is called anti-Stokes line as shown in fig 2.5 [8].

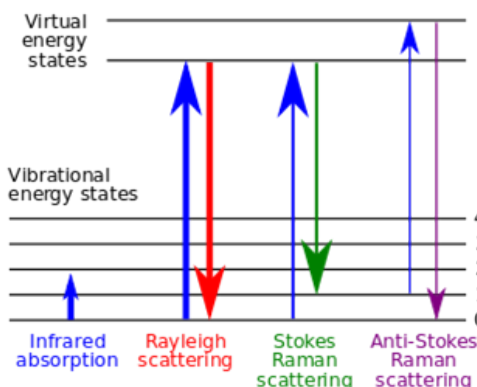


Figure 2.5: *Energy level diagram for various vibrational transitions (from Wikipedia).*

The molecules become Raman active only if they have polarisability. Raman band arises from an oscillating induced dipole caused by light waves interacting with the polarisability ellipsoid of the vibrating molecule.

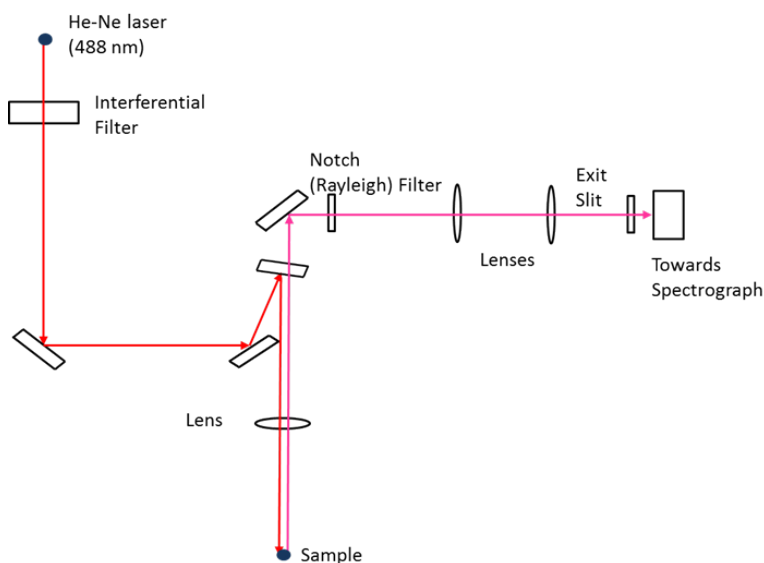


Figure 2.6: *Schematic diagram of Raman Spectrometer.*

The basic components of Raman spectrometer are shown in fig. 2.6. The illumination system consists of one or more lasers. The major restriction for the illumination system is that the incident frequency of light must not be absorbed by the sample or solvent. The laser light is directed to the sample using a combination of mirrors and lenses. The back scattered light from the sample is passed through the notch filter. Purpose of the notch filter is to remove Rayleigh scattered light and pass only the Raman scattered light. This filtered light is then passed through a series of lenses and the exit slit towards the spectrograph for further analysis.

In this project, Horiba Lab RAM HR instrument was used for recording Raman spectra of GO. Laser source having wavelength $488nm$ was used for all the measurements.

2.2.6 Four-Point Probe Method

The four-point probe is a tool for measuring resistivity of semiconducting materials. It can measure either bulk or thin film samples. The set up consists of four equally spaced metal tips with finite radius as shown in fig. 2.7. Current is supplied through the outer two probes and voltage is measured across the inner two probes for determining the sample resistivity.

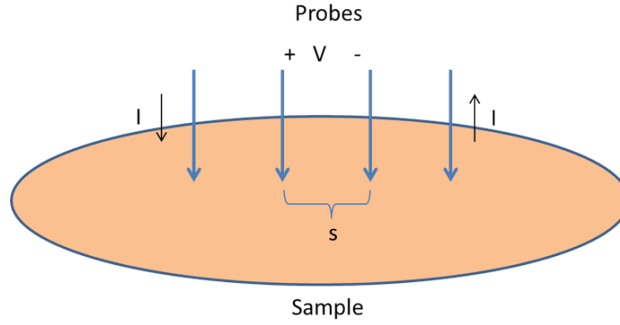


Figure 2.7: Schematic diagram of four-probe set-up.

The inner two probes draw no current because of the high input impedance voltmeter. Thus the contact resistance caused by the two probes and the sample can be eliminated.

At a constant temperature, the resistance, R of any conducting material is given by,

$$R = \rho \frac{L}{A}$$

Where ρ is the resistivity, L is the length and A is the area of cross section of the conductor. For bulk samples, thickness of sample (t) is much larger than the probe spacing (s). The bulk resistivity is derived by integrating the differential resistance between the inner probe tips and using Ohm's law ($V=IR$). The expression is given by

$$\rho = 2\pi s \frac{V}{I}$$

For a very thin layer (thickness $t \ll s$) we get current rings instead of spheres. The sheet resistivity is given by

$$\rho = k \frac{V}{I}$$

Where k is the geometric factor and in the case of a semi-infinite thin sheet, $k = 4.53$.

In this project, Keithley Four-Probe set-up was used for measuring the resistivity of thin films. The GO, RGO and Au NWs films were deposited on glass substrates for the measurement. The distance between the two probes was 2.4mm . So, the length of the films was kept to be more than 14mm^2 in order to make the contact between probes and the samples properly.

2.3 Bibliography

1. Libin Tang, Xueming Li, Rongbin Ji, Kar Seng Teng, Guoan Tai, Jing Ye, Changsong Wei and Shu Ping Lau, "Bottom-up synthesis of large-area graphene oxide nanosheets," *J. Mater. Chem.*, vol. 22, pp. 5676–5683, **2012**.
2. H. A. Becerril, J. Mao, Z. Liu, R. M. Stoltenberg, Z. Bao, and Y. Chen, "Evaluation of Solution-Processed Reduced Graphene Oxide Films as Transparent Conductors," *ACS Nano*, vol. 2, no. 3, pp. 463–470, **2008**.
3. H. Feng, Y. Yang, Y. You, G. Li, J. Guo, and T. Yu, "Simple and rapid synthesis of ultrathin gold nanowires , their self-assembly and application in surface-enhanced Raman scattering ," *Chem. Comm.*, pp. 1984–1986, **2009**.
4. <https://www2.chemistry.msu.edu/faculty/reusch/virttxtjml/spectrpy/uv-vis/uvspec.htm>.
5. <http://www4.nau.edu/microanalysis/Microprobe-SEM/Instrumentation.html>.
6. <http://cnx.org/content/m22326/1.4/>.
7. http://en.wikipedia.org/wiki/Fourier_transform_infrared_spectroscopy.
8. http://en.wikipedia.org/wiki/Raman_spectroscopy.

Chapter 3

Results and Discussions

As mentioned in chapter 1, transparent and conducting films (TCF) play a major role in revolutionizing the modern technology. They can be used in variety of areas. From the application point of view, there is a need for the replacement of the most commonly used indium tin oxide (ITO) as the TCF, because of their high cost and scarcity. Organic and metallic films are being explored extensively for this purpose. The aim of this project was to develop thin films separately from reduced graphene oxide (RGO) and gold nanowires (Au NWs) as well as a hybrid film of these two.

In this chapter, the results obtained in different experiments will be described. The characterization of GO films, obtained using different types of sugars will be discussed in the first part. The results for the reduction of GO will be explained in the next section. The subsequent part will be dedicated to the results obtained for Au NWs followed by the discussion of the results for hybrid GO/Au NWs films.

3.1 Graphene Oxide (GO)

Following the bottom up approach, large area GO was synthesized using hydrothermal synthesis[1]. As discussed in chapter 2, this is a very simple method which uses only sugar as the precursor. There are three reaction parameters (concentration of sugar solution, temperature of the reaction and time of reaction) which can be varied and films having different thickness can be obtained.

Initially, glucose ($C_6H_{12}O_6$) was used for the synthesis of GO films. The mechanism of the formation of films was discussed in chapter 1. During initial synthesis, very small flakes which were hardly visible were obtained. In the next 3-4 trials, the reaction conditions were optimized and very good GO films were synthesized. Upon initial observations, it was seen that GO films were brown in colour and were formed on the surface of the solution. Because of hydrophobic property, GO floats on the surface. The formation of the films was examined by keeping two reactions parameter constant and varying the other. In the first set of experiments, concentration of the glucose solution was kept $0.65M$ and the temperature $200^\circ C$. The time of the reaction was varied from $7h$ to $14h$. It was observed that as the time was increased, the thickness also increased. The reason being the polymerization of more number of glucose molecules to form a thicker film as the solution was kept for longer time. This variation is shown in table 3.1.

One more observation was the decrease in the lateral size of the films with the

decrease in time of the reaction. Upon visual observations, it was found that the $\sim 15nm$ films had lateral area of $1 - 9mm^2$ whereas the film having thickness $900nm$ was $> 1cm^2$ in area. Again the reason is that more number of glucose molecules polymerizes to increase the thickness as well as lateral area by increasing the time of reaction.

Time of reaction (hours)	Thickness of the film (nm)	Area of the film (mm^2)
7	~ 15	1-9
9	~ 90	< 50
12	~ 350	< 100
14	~ 900	> 100

Table 3.1: Results obtained during the synthesis of GO by keeping concentration of glucose solution $0.65M$, temperature $200^\circ C$ and varying the time of the reaction.

In the second set of experiments, the formation of films was studied as a function of temperature of reaction. The concentration of the reaction was kept to be $0.65M$ and the time was kept constant for $7h$. Temperature was varied from $160^\circ C$ to $200^\circ C$. No films were observed until temperature $185^\circ C$. But films of thickness $\sim 15nm$ were formed at $200^\circ C$. These results are listed in table 3.2.

Temperature ($^\circ C$)	Thickness of the film (nm)	Area of the film (mm^2)
160	–	–
175	–	–
185	–	–
200	~ 15	1-9

Table 3.2: Results obtained during the synthesis of GO by keeping concentration of glucose solution $0.65M$, time of the reaction $7h$ and varying the temperature.

Later in the project, in addition to glucose ($C_6H_{12}O_6$), lactose($C_{12}H_{22}O_{11}$), sucrose($C_{12}H_{22}O_{11}$) and galactose($C_6H_{12}O_6$) were used for the synthesis. In each case, brown films of GO were formed on the surface of the solutions as can be seen in fig. 3.1. The figure shows the formation of GO films using different sugars at different reaction conditions. Depending on the reaction conditions, films of different thickness and lateral area are produced which will be discussed next.

The comparison of GO films obtained from different sugars was done by keeping concentration and temperature of the reaction constant and varying the time of reaction. In particular, $0.325M$ sugar solutions were taken and kept in the autoclave at $190^\circ C$. The reaction time was varied from 4 hours to 7 hours. The results are listed in table 3.1. It was observed that, for the same reaction conditions sucrose and lactose gave films of greater thickness as compared to glucose and galactose. This happens because glucose and galactose are monosaccharide whereas sucrose and lactose are disaccharide i.e. they are formed by the condensation of two monosaccharides. So monomers for GO in the case of disaccharides are larger than monosaccharides leading to thicker films.

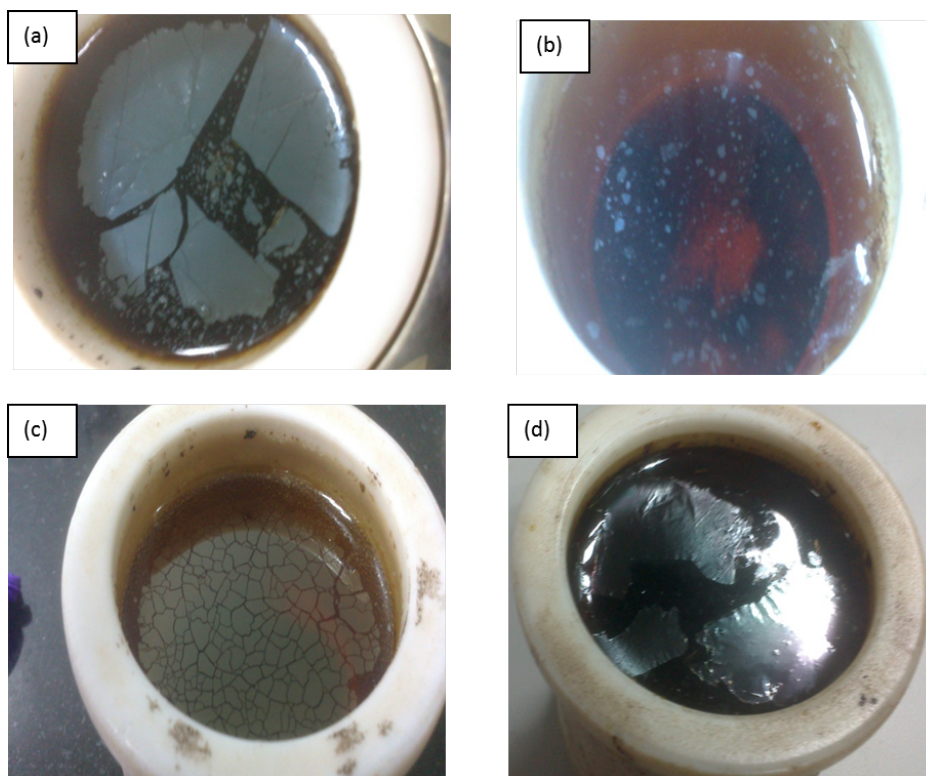


Figure 3.1: *Optical images of GO formed on the surface of the solution using (a) glucose (b) galactose (c) lactose (d) sucrose.*

There were no films produced from glucose and galactose for reaction times less than and equal to 6 hours. However, sucrose solution gave films for all the reaction time from 4 to 7 hours. For lactose, films were formed for reaction time greater than 6 hours.

Some of the thin GO films remained wet and could not be dried even after many trials. Because of this, their thickness could not be measured since the film was not distinguishable from the solvent. This might have happened because of the H-bonding between water molecule and the oxygen containing functional groups.

Area according to the visual observation (A) and the thickness (T) of GO films produced from different sugars

Time(h)	Glucose (A,T)	Galactose (A,T)	Sucrose (A,T)	Lactose (A,T)
7	< 10mm ²	10 – 20mm ² , ~ 350nm	> 1cm ² , ~ 900nm	< 25mm ² , ~ 500nm
6	No film	No film	< 0.25cm ²	< 5mm ²
5	No film	No film	< 25mm ²	No film
4	No film	No film	< 25mm ² , ~ 400nm	No film

Table 3.3: *Results obtained for the synthesis of GO using different sugars (keeping temperature and concentration of sugar solution constant and varying the time)*

3.1.1 AFM analysis

The thickness of the synthesized films was measured by AFM. The films were deposited on the silicon substrate and dried. Under the microscope, the edges of the

films were scanned such that image contained film as well as the substrate. From the height profile of such images, the thickness was measured. Some of the AFM images of GO produced from glucose and their height profiles are shown in fig. 3.2.

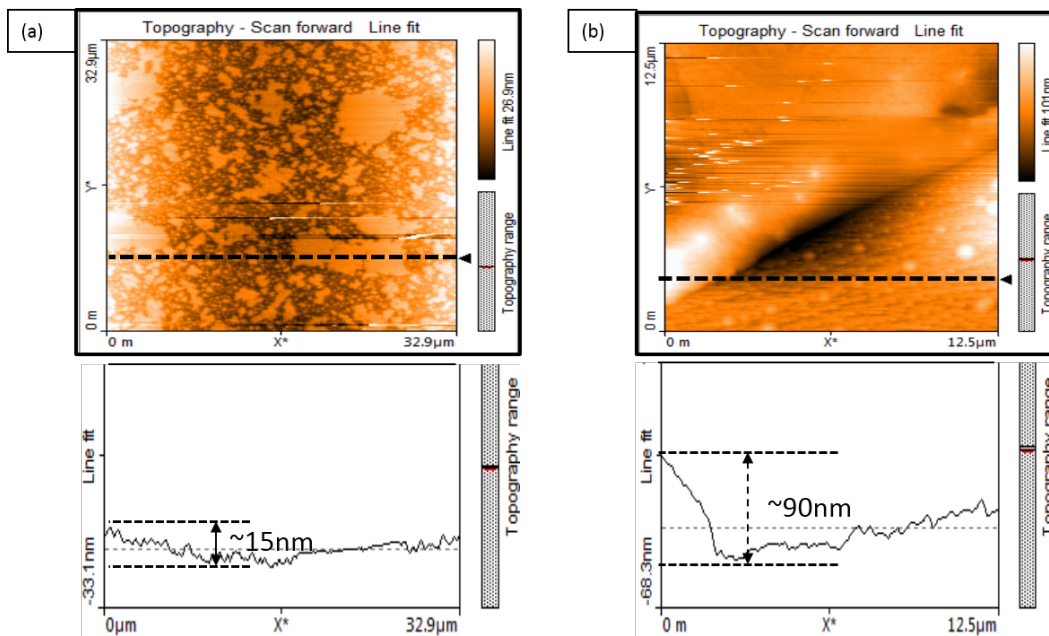


Figure 3.2: AFM images and height profiles (corresponding to the dotted black line in the AFM image) of GO synthesized from glucose for reaction conditions (a) Concentration=0.65M, T=200°C, time=7h (b) Concentration=0.65M, T=200°C, time=9h.

As discussed in previous section, the thickness of GO films prepared from glucose increased with increasing time of reaction. This was confirmed by the AFM images. Fig. 3.2 (a) shows the GO films prepared from 0.65M glucose solution at the temperature of 200°C kept for 7 hours. In fig. 3.2 (b), GO film prepared at same reaction conditions as previous but with increased time, is shown. As expected, the thickness was more GO prepared, by keeping the glucose solution for 9 hours. The thicknesses of the films are $\sim 15nm$ and $\sim 90nm$ respectively.

Fig. 3.3 shows the AFM images of GO films prepared from different sugars. The figure also shows height profiles of the AFM images corresponding to the black dotted lines. These films did not have uniform thickness throughout the sample, so images were taken at various places and average thickness was calculated. The film obtained from galactose has an average thickness of $\sim 350nm$ for reaction conditions: concentration=0.325M, T=190°C, time=7h. Average thickness of films prepared from glucose for reaction conditions: concentration=0.65M, T=200°C, time=12h is $\sim 350nm$. Lactose and sucrose solutions give film of average thickness $\sim 500nm$ and $900nm$ respectively for reaction conditions: concentration=0.325M, T=190°C, time=7h.

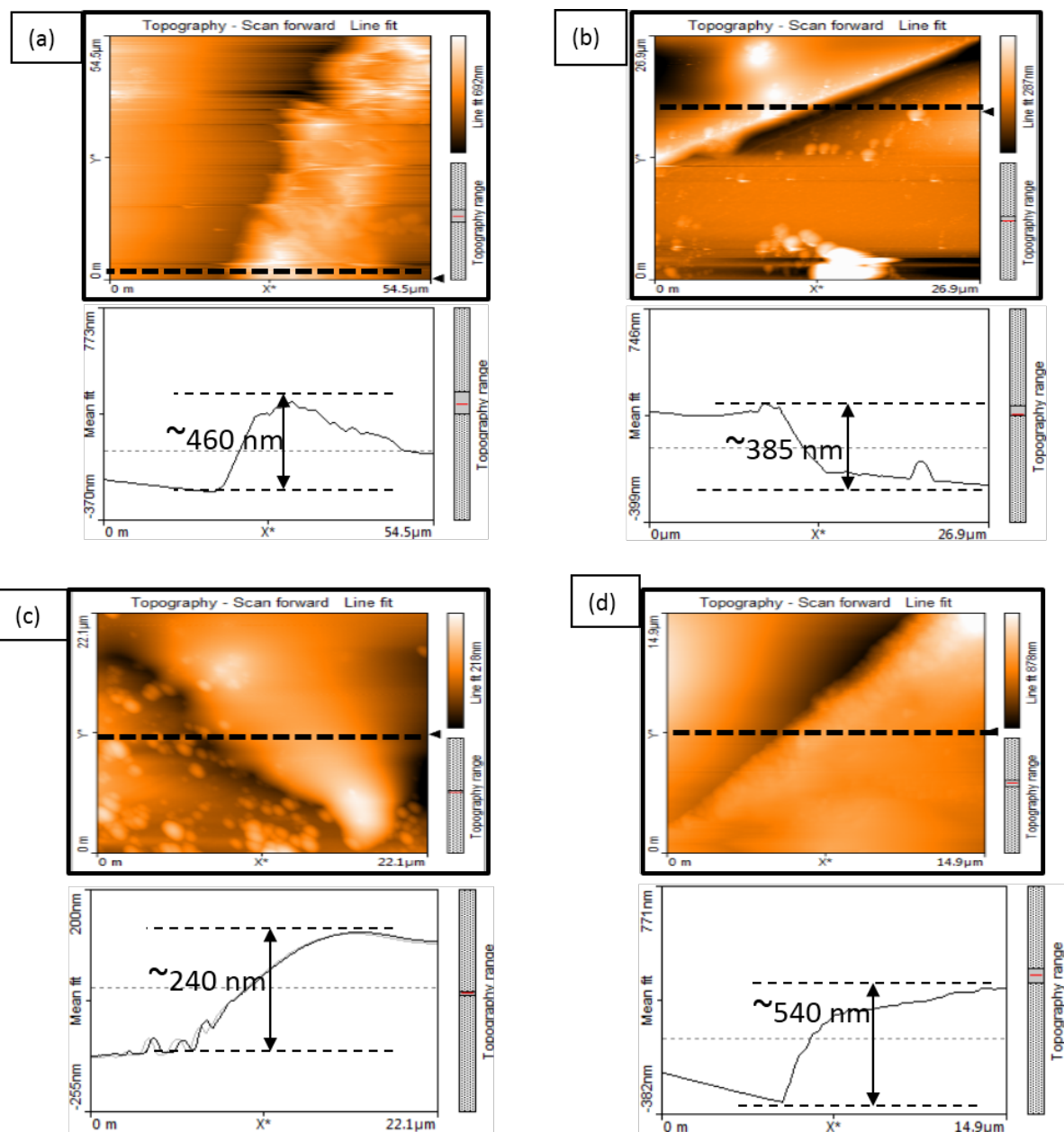


Figure 3.3: *AFM image and height profile (corresponding to the dotted black line in the AFM image) of GO films prepared from (a) galactose (b) glucose (c) lactose (d) sucrose*

3.1.2 SEM analysis

For studying the morphology and the uniformity of the films, SEM images were taken. Samples were prepared as described in chapter 2. The images were taken for the same samples for which AFM images were recorded (discussed in the last section).

For GO, obtained from 0.65M glucose solution with reaction temperature 200°C and time of 12h, very uniform films were obtained. As can be seen in fig. 3.4 (a), the film has area $\sim 1.7mm^2$ without any break.

Film prepared from galactose with reaction conditions: concentration=0.325M, temperature=190°C and time=7h, has area of $\sim 0.07mm^2$ with no breaks. GO

film obtained from galactose is shown in fig. 3.4 (b).

Fig. 3.4(c) shows the GO film obtained from lactose at reaction conditions: concentration= $0.325M$, temperature= $190^{\circ}C$ and time= $7h$. The film has lateral area $\sim 0.4mm^2$. However it has several breaks.

In Fig. 3.4(d), GO film synthesized from lactose is shown. The reaction conditions were: concentration= $0.325M$, temperature= $190^{\circ}C$ and time= $7h$. Film thus obtained shows lateral area $\sim 0.8mm^2$ and several breaks in between.

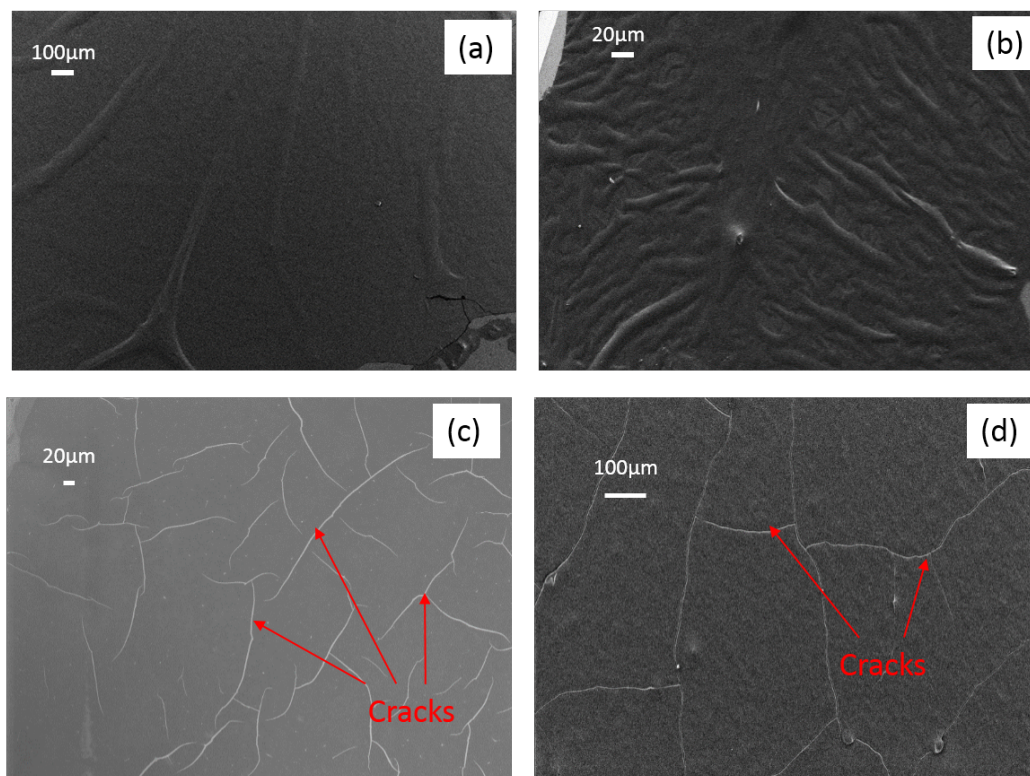


Figure 3.4: SEM images of GO obtained from (a) glucose (b) galactose (c) lactose (d) sucrose.

3.1.3 FTIR analysis

For determining the types of bonds present in GO prepared from different sugars, Fourier transform infrared spectroscopy (FTIR) was carried out. All the samples showed the presence of same kind of bonds as can be seen from the FTIR spectra in fig 3.5. The O-H bond indicates the functional groups such as hydroxyl and carboxylic acid. The C=O bond corresponds to the functional groups like carboxylic acids, esters and ketones and C-O corresponds to ester, epoxy and carboxylic acid. In these bonds, the carbon atom is sp^3 hybridized. Also C-H and C=C bonds are observed in the spectra. The C=C bonds are present at the edges of the GO sheets in which carbon atoms are sp^2 hybridized and no functional groups are attached to them. C-H bonds are also present at the edges where carbon atoms are present in the sp^2 hybridized state, however these carbon atoms may or may not be attached to the functional groups (fig. 1.4).

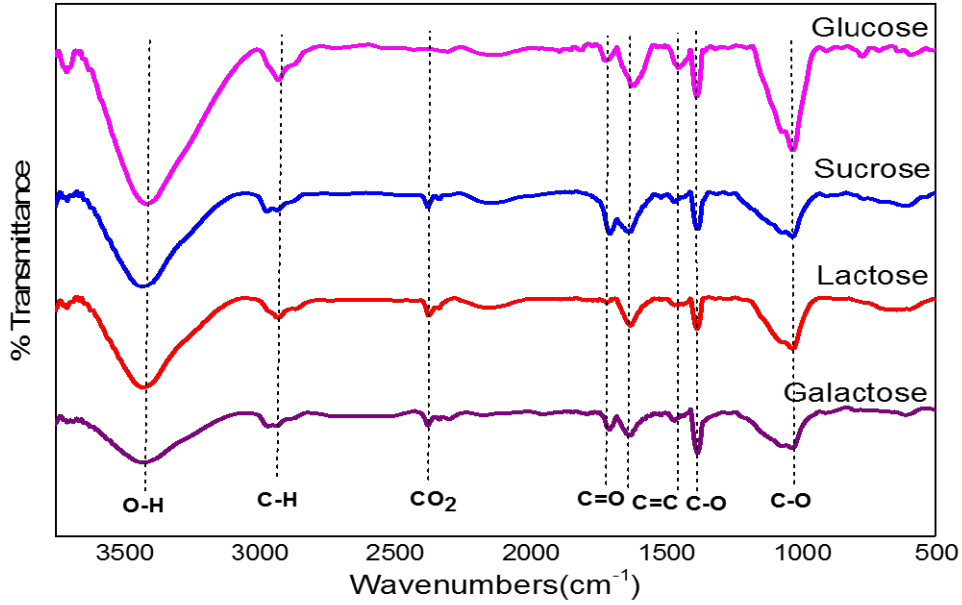


Figure 3.5: *FTIR spectra of GO obtained from different sugars.*

3.1.4 Raman analysis

Raman spectroscopy was carried out to find out different kinds of vibrational modes present in the GO sheets. Typical Raman spectrum of GO shows two bands: D band and G band. The G band corresponds to the first-order scattering of in plane tangential stretching mode, while the D band, also called as disorder band, originates from disorder in the sp^2 hybridized carbon atoms, characteristic for lattice distortions in the GO sheets. Different vibrational modes in the sp^2 ring of GO are shown in fig. 3.6 (a) and (b). The ratio of the intensity of D band and G band $\left(\frac{I_D}{I_G}\right)$ gives a measure of disorder in the GO films. Higher the value, less will be the defect[2].

The Raman spectra of GO obtained from different sugars are shown in fig. 3.6. For GO prepared from glucose, D band and G band were observed at $1379cm^{-1}$ and $1595cm^{-1}$ respectively. And ratio of the intensity of D band and G band i.e. $\frac{I_D}{I_G}$ was equal to 0.72. The D band and G band of GO synthesized from lactose were observed at $1378cm^{-1}$ and $1583cm^{-1}$. Ratio $\frac{I_D}{I_G}$ came to be 0.595. GO prepared from sucrose, showed D band at $1369cm^{-1}$ and G band at $1593cm^{-1}$ with $\frac{I_D}{I_G} = 0.608$. The Raman spectra for GO obtained from galactose could not be recorded as it was showing fluorescence. The observed fluorescence in the Raman spectra might be because of the two reasons. First reason can be the high energy laser source (488nm) used which is sufficient to cause electronic transitions in the absorbing species and remission at longer wavelength. Net result is the envelope of fluorescence upon which Raman signal show up. The other reason for the absence of the Raman signal, for

GO synthesized from galactose might be due to the very small flakes of sample.

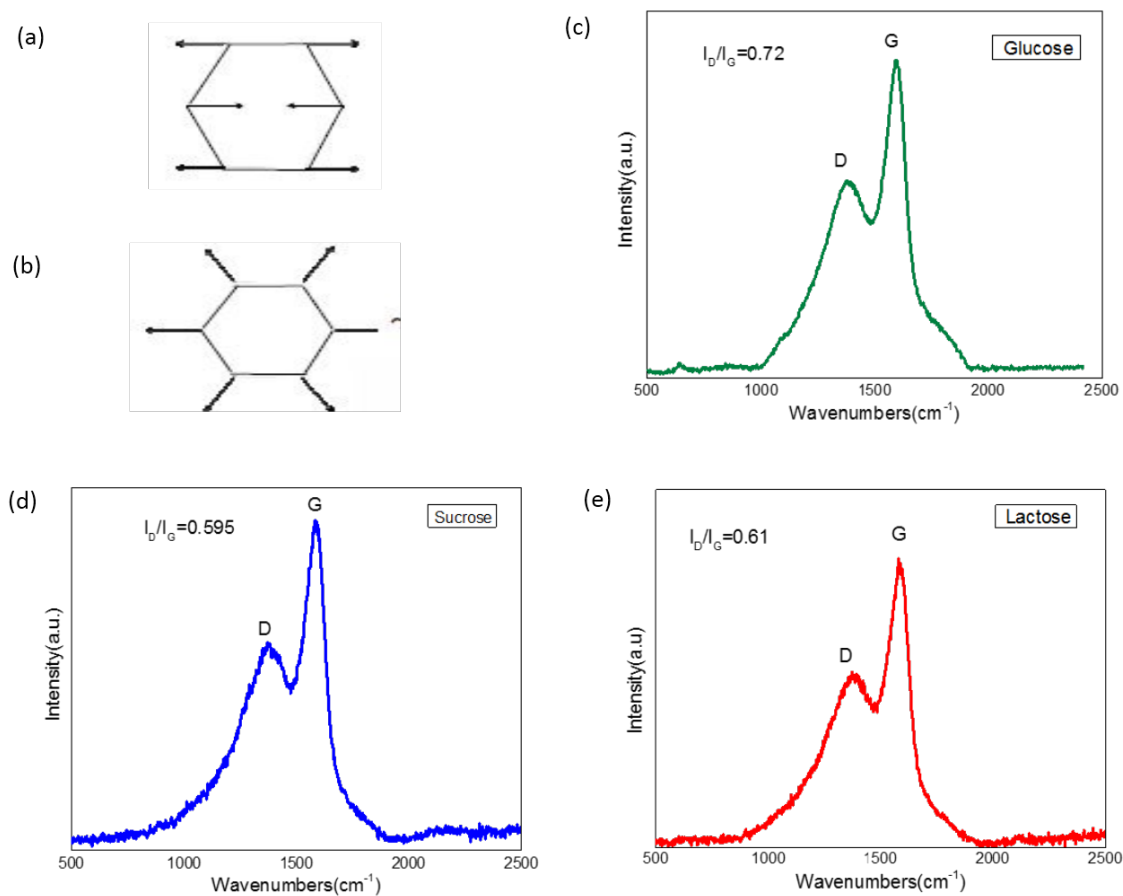


Figure 3.6: (a) G mode (in plane vibration of sp^2 ring) (b) D mode (vibration due to the disorder at the edges of the ring). Raman spectra of GO obtained from (c) glucose (d) sucrose (e) lactose.

3.2 Reduction of GO

The reduction of GO was done by a combination of chemical reduction using hydrazine and thermal reduction as discussed in chapter 2 [3]. Upon initial observation, the colour of GO film changed from brown to metallic gray after chemical reduction. After thermal reduction, the colour changed to black. For the confirmation of reduction, FTIR and Raman spectroscopy was carried out.

3.2.1 FTIR analysis

From the FTIR spectra given in fig. 3.7, it can be observed that, RGO does not contain C-O and C=O bonds in contrast to GO. This indicates the removal of functional groups such as epoxy, ketones and carboxylic acids. Since the oxygen

containing functional groups are reduced, the sp^2 network is getting restored. This leads to the increase in conductivity of GO which will be discussed in section 3.5.

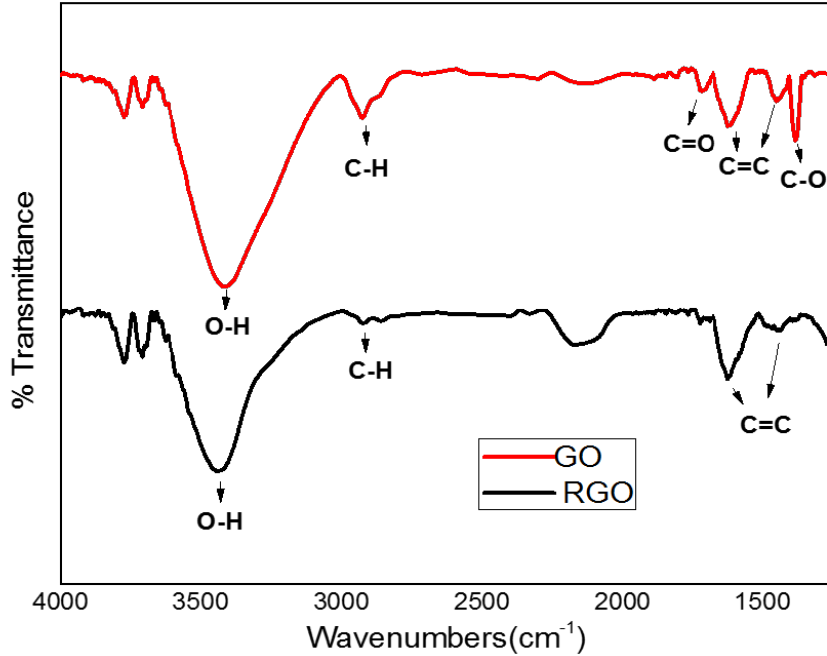


Figure 3.7: FTIR spectra of GO and RGO

3.2.2 Raman analysis

Raman spectroscopy also confirmed the reduction of GO. As reported in the literature, the ratio $\frac{I_D}{I_G}$ increases for RGO compared to GO[4]. The increased $\frac{I_D}{I_G}$ value in case of RGO is due to the removal of oxygen functional groups in GO sheets and the reestablishment of a conjugated graphene network. The reestablished graphene network usually has a smaller average size than the original graphite oxide, which leads to a consequent increase in the intensity ratio $\frac{I_D}{I_G}$. It can be seen in fig. 3.8 (pink), the characteristic D and G bands for GO are observed at $1379cm^{-1}$ and $1599cm^{-1}$, respectively, and a D/G intensity ratio of 0.61. The RGO spectrum (Fig. 3.8 (blue)) shows a slightly shifted G-band and D-band peaks towards lower values at $1372cm^{-1}$ and $1577cm^{-1}$, and an increased D/G intensity ratio of 0.72 and thus confirming the reduction.

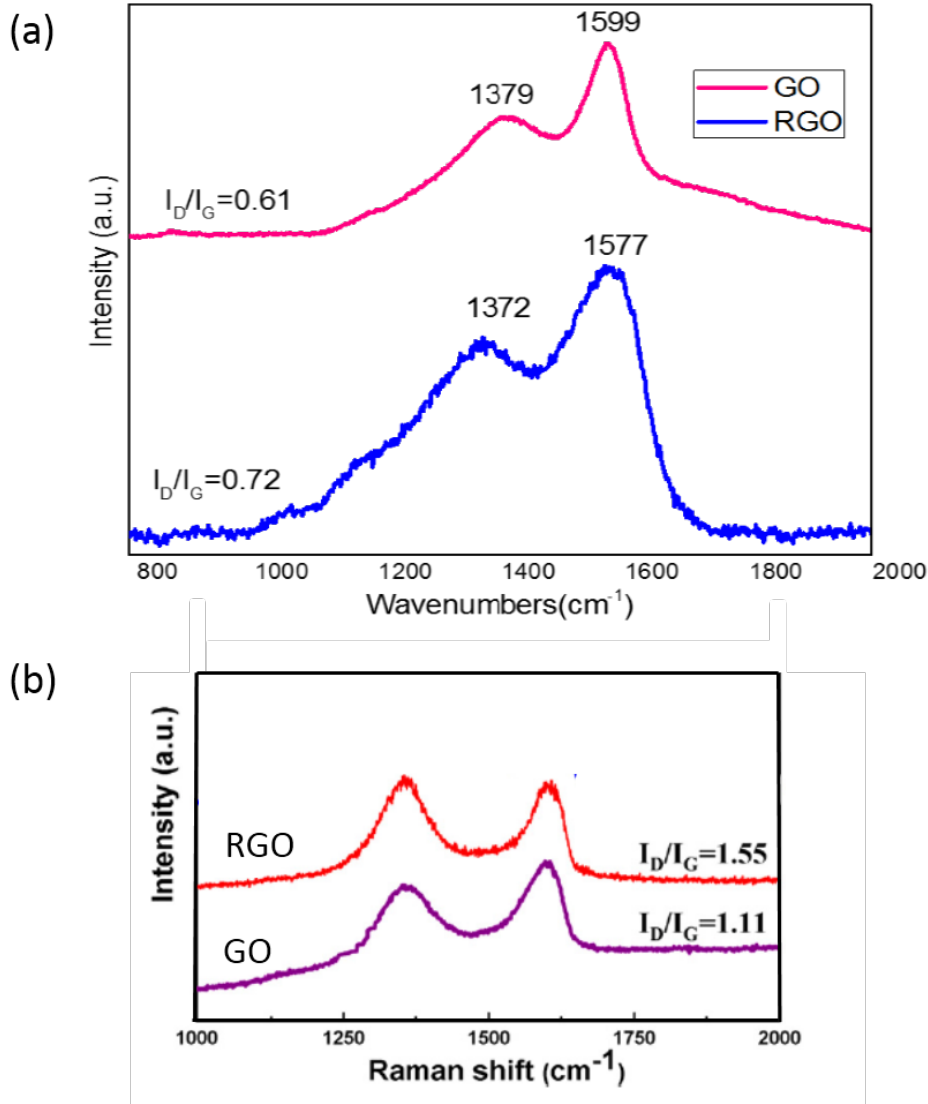


Figure 3.8: Raman Spectra of GO and RGO (a) obtained (b) from literature[4].

3.3 Gold Nanowires (Au NWs)

Au NWs were synthesized following the wet chemical method as described in chapter 2 [4]. When oleylamine (OA) is added to gold chloride($AuCl_3$), a complex formation takes place. And due to the aurophilic interactions, these complexes come close together and form a polymeric chain. Aurophilic interactions are the interactions between gold atoms when they come very close to each other. These interactions are similar to H-bonding interactions. When triisopropylsilane(TIPS) is added, it reduces the $Au(III)$ to $Au(0)$ leaving behind the ultrathin Au NWs. These nanowires have OA as the capping agent, which prevents them from aggregating. The mechanism of the formation of Au NWs is shown in fig. 3.9.

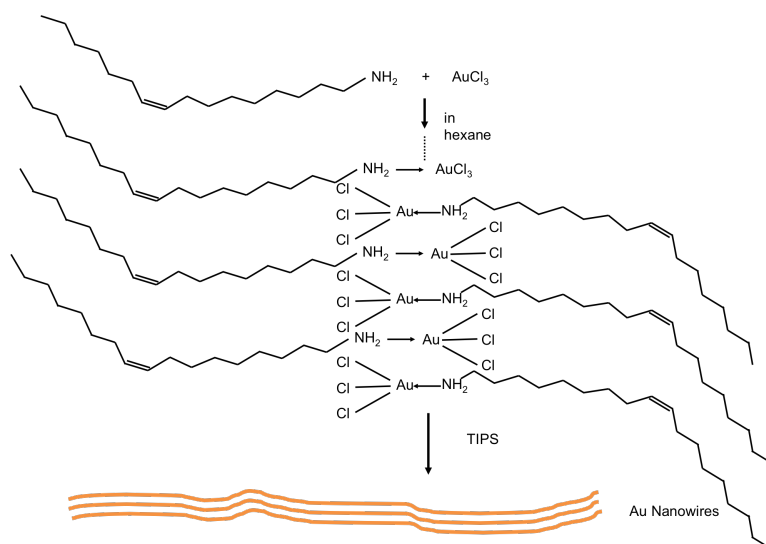


Figure 3.9: Mechanism of Au NWs formation : Complex is formed between OA and AuCl_3 , followed by the reduction of Au(III) to Au(0) by TIPS and finally leading to the formation of nanowires.

3.3.1 SEM analysis

To see the morphology of nanowires produced, SEM images were taken. The Au NWs solution was drop-casted on silicon substrate and dried. As can be seen in the fig. 3.9, ultrathin nanowires with very good morphology were produced. The thickness of nanowires was found to be in the range $5 - 50\text{nm}$ and length in micrometers. Due to the intertwinement of nanowires, the exact length could not be measured as the two ends for single wires were not distinctly visible. Also because of the limited resolution of SEM, it was not confirmed that the larger thickness of wires was because of increase in diameter of the wires or due to the clumping of thinner wires.

The nanowires were very uniform in nature. It was also observed that the nanowires self-assembled themselves parallel to each other in a 2D network. Reason behind this alignment is the hydrophobic interaction between alkyl chains of OA on the nanowires [5].

Formation of nanowires was studied as a function of reaction time. Fig 3.10 shows wires formed by keeping the solution for different times. It was observed that very small and thin wires having rough morphology were formed for reaction time of 4h along with lots of nano particles. This suggests the initial stage of formation of wires. As the solution was kept for longer time, the wires with good morphology and longer length were produced. However, the aspect ratio of the wires could not be measured as they formed loop kind of structures and the two ends for a single wires were not identifiable in the FESEM images. Also, the number of nanoparticles was reduced and for 14h reaction, there were no particles at all. The increased reaction time produced uniform wires, which self-assembled parallel to each other as explained above.

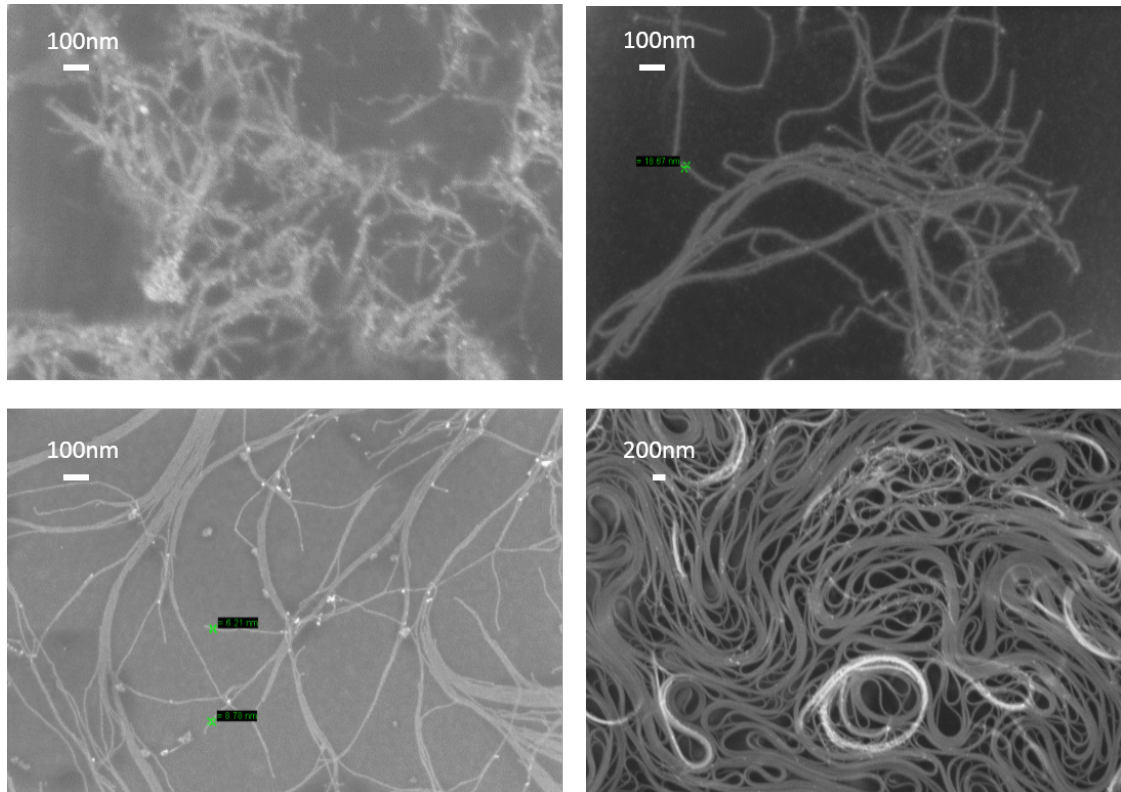


Figure 3.10: SEM images of Au NWs for reaction time (a) 4h (b) 7 h (c) 12h (d) 14h.

3.3.2 UV-Vis absorption analysis

Solution phase UV-Vis spectroscopy of Au NWs was carried out to study the interaction of wires with the visible light. After interacting with the electromagnetic radiation, collective oscillation of surface electrons occurs perpendicular to the length of wire as discussed in section 1.5.1. Due to this, absorption of visible light takes place at $\sim 520nm$ corresponding to the transverse surface plasmon (TSP) resonance peak. The position of the TSP peak depends upon the aspect ratio of wires. Fig. 3.11 shows a blue shift in the TSP peak with increasing time of reaction, indicating the increase in aspect ratio. The peak shifted from $532nm$ to $511nm$ for the reaction time increasing from 4h (green line) to 14h (black line).

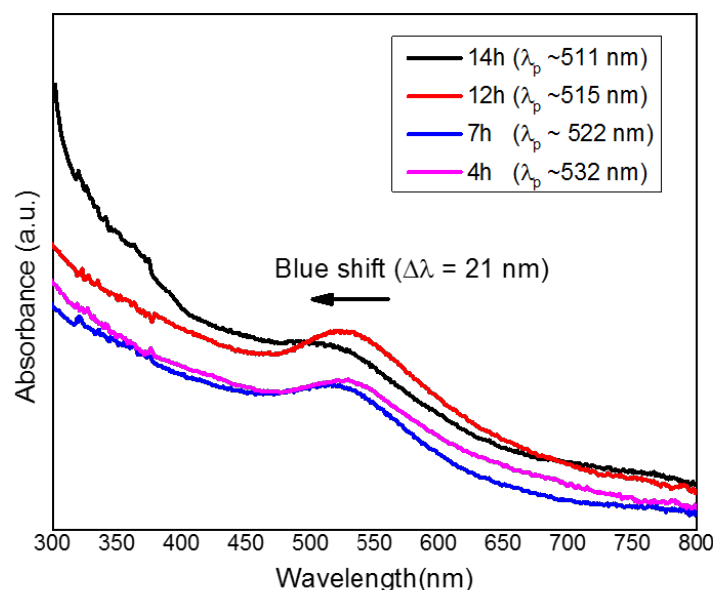


Figure 3.11: *UV-Vis spectra of Au NWs for different reaction times.*

3.4 Hybrid film of GO/Au NWs

A hybrid nanostructure is formed by the composition of two or more nanostructures. These hybrid structures can be nanorods attached to a nanoparticle tip, core-shell particles in which core is made up of one material and the shell is made up of another material, hybrid films in which two nanofilms are alternatively stacked on top of each other and so on. The idea behind producing hybrid nanostructures is to achieve properties which are combinations of the component structures. Some new properties can also be attained because of the interaction between the constituent nanostructures.

In the project, the motivation for synthesis of hybrid film of GO/Au NWs was to get films with better conductivity. The Au NWs were intercalated with GO films with the expectation that these nanowires will contribute to the conduction of electrons and increase the conductivity. The hybrid film of GO/Au NWs was prepared following the procedure described in chapter 2. The GO film deposited on the silicon or glass substrate was put in the growth solution of Au NWs. Initial observations indicated the change in colour of GO film from brown to reddish brown. From the SEM images (fig. 3.12) it was observed that gold nanowires formed another layer on the surface of GO. These wires were present on the GO surface even after washing with ethanol and hexane which indicated some kind of binding between GO and Au NWs. However, this observation has not been confirmed yet by any of the characterization techniques.

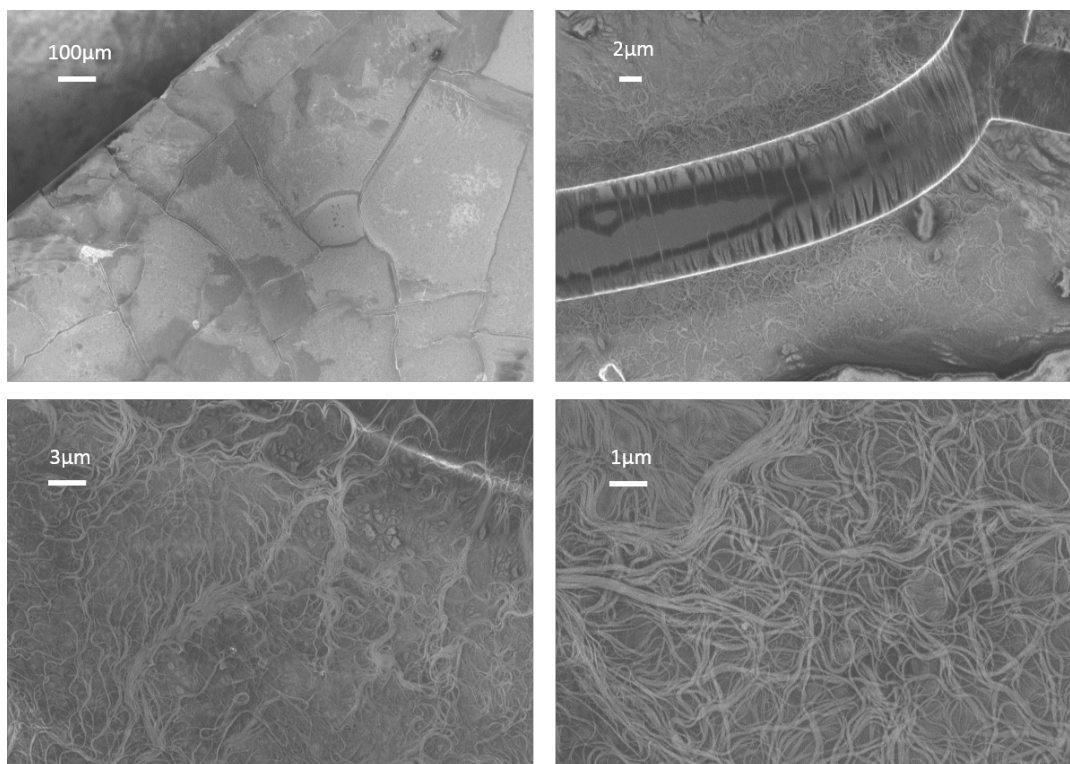


Figure 3.12: SEM images of layer of Au NWs on top of GO film.

In order to check any kind of bonding between GO and Au NWs, FTIR spectra was recorded for the hybrid film as shown in fig. 3.13. It was observed that spectra had similar peaks as that of GO. The peaks for O-H, C-H, C=O, C=C and C-O were present in the spectrum. However no conclusion could be drawn for the binding between nanowires and the GO film from this spectra.

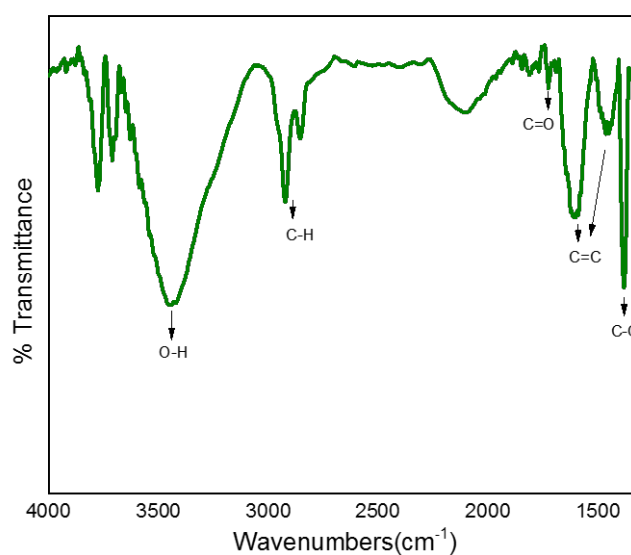


Figure 3.13: FTIR spectra of GO/Au NWs hybrid film.

3.5 Transparency measurements of films

The transparency measurement was carried out for the films prepared from GO and Au NWs. The transmittance of the films was recorded in the range 400 – 800nm by solid state UV-Vis spectroscopy.

The Au NWs film was prepared by drop-casting 20 μ L of the solution on glass slide and drying it. The thicker films were prepared by adding Au NWs solution in the step of 20 μ L. Subsequently, the transmission was recorded. The exact thickness of the films could not be measured because of the limited resolution of the AFM used. The transparency was found to be >80% for all the films as shown in fig. 3.14. As expected, the thinner films were more transparent compared to the thicker films.

Also there is a dip in all the peaks at ~520nm. This is because of the TSP resonance of the Au NWs as discussed in section 3.2.2. It is observed that, as the thickness of film is increasing, the intensity of the dip is also increasing. This can be explained by the increased number of Au NWs which absorb the visible radiation due to TSP resonance in the thicker films.

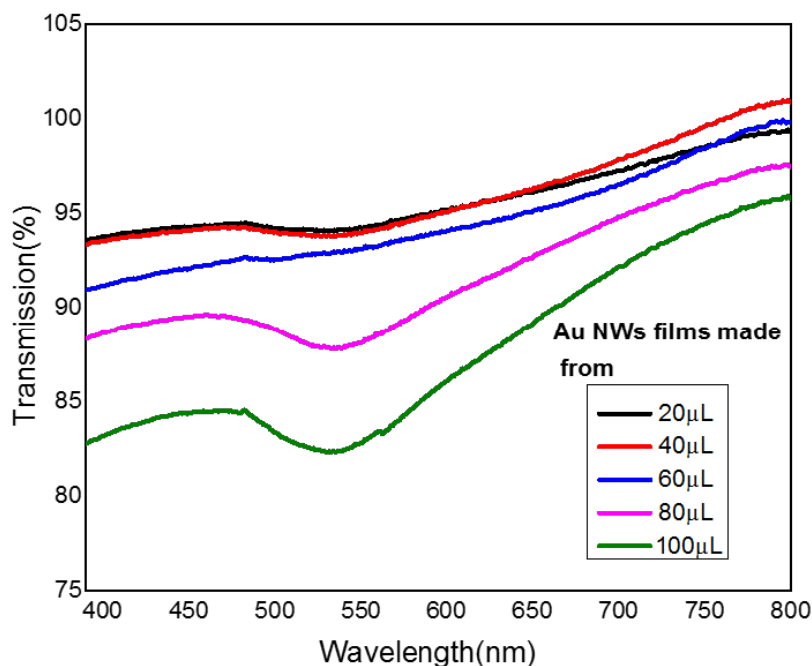


Figure 3.14: *Transmission spectra of Au NWs films of different thicknesses.*

The transmission of GO films was also recorded in the range 400-800nm. The spectra are shown in fig. 3.15. Films with greater thickness were less transparent as compared to thinner films as expected. In particular, the transparency for the films was compared at 550nm by comparing the percent transmission at this wavelength. Film having thickness 800nm was least transparent with transmission of 10% at 550nm. Transmission of 28% was observed for the film of 500nm at the same

wavelength. The thinnest film of these three films, having thickness 100nm , showed 70% transmission.

However, the transparency of films with even smaller thickness could not be measured. The solid state UV-Vis spectroscopy needs a minimum area of the sample for which spectra needs to be recorded and thin GO films ($<100\text{nm}$) had small area which was not sufficient for the measurement. Later, the plan is to exfoliate thin GO films from thicker films and make large area films with smaller thickness. The hope is that these films will be more transparent.

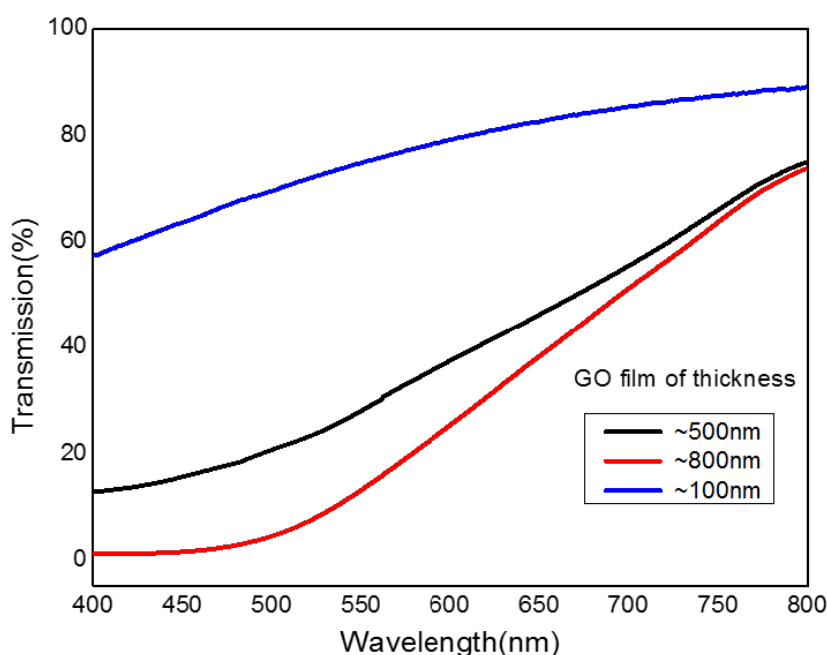


Figure 3.15: *Transmission spectra of GO films.*

The transparency of the hybrid GO/Au NWs films could not be measured for the same reason, as discussed above about thin GO films. Even though large area GO films were taken during the synthesis of hybrid film, the films broke once they were put in the growth solution of Au NWs. So small flakes of hybrid film were obtained which were not sufficient for the transparency measurement.

The experiments for making hybrid film, using exfoliated GO and Au NWs solution, having larger area are in progress. The expectation is to get thin hybrid films with large area, which are also transparent.

3.6 Conductivity measurement of films

The conductivity of the films prepared from GO and Au NWs was measured using Four-probe set-up. The films were deposited on the glass substrate and measurement

was carried out at room temperature. The area of the film prepared was more than 50mm^2 , as the distance between the two outer probes was 7.2mm with inter spacing of 2.4mm between the adjacent probes. Varying current from 10^{-9} to 10^{-12} A was passed through the sample and corresponding voltage was measured.

The GO films produced were insulating having very high sheet resistance of the order of $10^9\Omega/\text{sq}$. This can be explained by the structure of GO. As discussed in chapter 1, GO has several oxygen containing functional groups attached to it. The carbon atoms, to which these functional groups are attached, exist in the sp^3 hybridization having no π -electrons. This leads to disruption in the conjugation of π -electrons of the sp^2 hybridized carbon atoms. Thus GO is non-conducting in nature.

Functional groups are removed by the reduction of GO (as discussed in chapter 2). After removal of the functional groups, the carbon atoms change its hybridization from sp^3 to sp^2 and hence the π -networks are restored. This makes RGO conducting. After reducing GO film (thickness= 500nm) with hydrazine and annealing it at 400°C , the sheet resistance decreased from $10^9\Omega/\text{sq}$ to $10^7\Omega/\text{sq}$. It has been reported that after hydrazine treatment and thermal annealing, the sheet resistance as small as $10^3\Omega/\text{sq}$ can be achieved for 30nm film[3]. However, here such small sheet resistance could not be achieved because of the larger thickness. Even though films of smaller thickness ($\sim 15\text{nm}$) were synthesized, their area was not sufficient for the four probe measurement. Further, for reducing the thickness, the exfoliation of GO films is being carried out and later large area films of thin GO flakes will be made. The reduction of these films will be carried out for the better conductivity.

The sheet resistance of Au NWs films was also measured. It was observed that films had very high sheet resistances of the order $10^9\Omega/\text{sq}$. This high value of sheet resistance might be due to the two reasons: capping agent and contact resistance at the joint of wires [5]. One possible way to decrease the sheet resistance could be the removal of capping agent from the surface of nanowires. The removal of the capping agent is planned to be done by plasma treatment and the work is in progress with the expectation of positive results.

The sheet resistance of hybrid GO/Au NWs film could not be measured because of smaller area of the films. The plan is to make large area exfoliated GO thin films, reduce them and then make the hybrid with Au NWs following the procedure given in chapter 2. Later, removal of capping agent is to be done by the plasma treatment. The hybrid film with better conductivity is expected.

3.7 Summary

In summary, this chapter was dedicated to the results obtained in various experiments carried out during the project. In the first two sections, the topic of discussion was GO and its reduction. The results obtained in the characterization of GO and RGO by techniques like SEM, AFM, FTIR and Raman Spectroscopy were discussed in these sections. In the next section the results obtained for Au NWs were described followed by the results of hybrid film of GO/Au NWs. In the last two sections, more was discussed about the transparency and conductivity of the films synthesized from GO and Au NWs.

3.8 Bibliography

1. Libin Tang, Xueming Li, Rongbin Ji, Kar Seng Teng, Guoan Tai, Jing Ye, Changsong Wei and Shu Ping Lau, "Bottom-up synthesis of large-area graphene oxide nanosheets," *J. Mater. Chem.*, vol. 22, pp. 5676–5683, **2012**.
2. D. Gournis and R. J. D. Miller, "Revealing the ultrafast process behind the photoreduction of graphene oxide," *Nat. Commun.*, pp. 1–5, **2013**.
3. H. A. Becerril, J. Mao, Z. Liu, R. M. Stoltenberg, Z. Bao, and Y. Chen, "Evaluation of Solution-Processed Reduced Graphene Oxide Films as Transparent Conductors," *ACS Nano*, vol. 2, no. 3, pp. 463–470, **2008**.
4. Zhenyuan Ji1, Xiaoping Shen, Minzhi Li, Hu Zhou, Guoxing Zhu and Kangmin Chen, "Synthesis of reduced graphene oxide/ CeO_2 nanocomposites and their photocatalytic properties", *Nanotechnology*, vol. 24, **2013**.
5. H. Feng, Y. Yang, Y. You, G. Li, J. Guo, and T. Yu, "Simple and rapid synthesis of ultrathin gold nanowires , their self-assembly and application in surface-enhanced Raman scattering ," *Chem. Comm.*, pp. 1984–1986, **2009**.
6. Y. Chen, Z. Ouyang, M. Gu, and W. Cheng, "Mechanically Strong , Optically Transparent , Giant Metal Superlattice Nanomembranes From Ultrathin Gold Nanowires," *Adv. Mater.*, vol. 25, pp. 80-85, **2013**.

Chapter 4

Conclusions and Future Directions

In this project, thin films from graphene oxide (GO), gold nanowires (Au NWs) and a hybrid of these two were synthesized. Large area GO was synthesized by a very novel and simple hydrothermal synthesis using only sugars as the sole reagent. Initially glucose was used for the synthesis of GO films. To obtain uniform films, the reaction parameters were optimized and after 3-4 trials GO was successfully synthesized. The variation in the thickness of films was studied by keeping two of the reaction conditions constant and varying the other. In the first set of experiments, after several trials 4 films were synthesized by keeping concentration and temperature of reaction and time was varied. It was found that with increasing time, the thickness of the film increased from ~15 nm to ~900 nm. In the second set, 4 more experiments were carried out by keeping concentration and time of the reaction constant and temperature was varied. It was observed that GO films start forming only after certain temperature for the given concentration and time of reaction.

Later, other sugars (galactose, lactose and sucrose) were used for synthesizing GO. A set of 16 experiments were carried out to study the formation from different sugars. For all the reactions, temperature and concentration of the sugars were kept constant and time was varied. For a given set of reaction conditions, the GO films obtained from different sugars were compared. It was found that lactose and sucrose being disaccharides gave thicker and larger area films compared to glucose and galactose which are monosaccharides. Further characterizations confirmed the formation of GO. SEM images showed the formation of large area films (as large as 1.7 mm^2). Thickness of the film was measured by AFM. FTIR spectroscopy confirmed the presence of different oxygen containing functional groups such as hydroxyl, epoxy, esters, ketones and carboxylic acids. Raman spectroscopy showed the two characteristic bands G-band and D-band corresponding to the in plane vibration of carbon network and vibrations at the edges. Reduction of GO was also carried out by a combination of chemical and thermal reduction. This was confirmed by the extinction of different peaks corresponding to the oxygen containing functional groups, in the FTIR spectra. In addition, the increase in the intensity ratio of D-band and G-band also confirmed the reduction of GO.

Au NWs were also synthesized following another simple wet chemical approach. The formation of wires was studied by carrying out several experiments with increasing reaction time (from 4h to 14h). SEM images showed the formation of very uniform ultrathin nanowires (thickness in range 5-50 nm) with very good morphology for larger reaction time. UV-Vis spectroscopy indicated the absorption of visible

light around 520 nm because of the transverse surface plasmon resonance. Later, these ultrathin Au NWs were repeatedly synthesized for preparing thin films. Hybrid film of GO/Au NWs was also synthesized using a self devised method. The formation of the hybrid film was confirmed by the SEM images which showed the layer of Au NWs on top of GO sheet.

The transparency and conductivity measurements were carried out for these films. All the transparency measurements were carried out for the wavelength range of 400-800 nm. GO films were found to be having different transparencies for different thicknesses. The transparency upto 90% was achieved for these films (for film of thickness ~ 100 nm). The films made from Au NWs were even more transparent having transparency upto 97%. The conductivity measurement for these films were carried out using Four-point probe method. The measurements indicated that as synthesized GO was an insulator having sheet resistance of $10^9 \Omega/sq$. This was due to the disruption of π -conjugation caused by the presence of the functional groups. To increase the conductivity of GO, reduction was carried out and it was found that the sheet resistance was reduced by the order of 2 giving the sheet resistance of $10^7 \Omega/sq$. The Au NWs films also showed high sheet resistance of the order $10^9 \Omega/sq$ because of the capping agent and the contact resistance between the wires. The transparency and conductivity measurements of hybrid films are in progress.

The plan for future is to optimize the transparencies and conductivities of the above synthesized films. In order to get better transparency and conductivity for the GO films, the thickness should be decreased. For this purpose, exfoliation is being carried out for GO films. Later these will be used for making large area films and will be reduced for better conductivity. The conductivity for Au NWs film can be increased by removing the capping agent attached to the nanowires. This experiment is in progress and positive results are expected. Also the experiments for making hybrid films with large area have been planned and are in progress. Later the transparency and conductivity of these films will be measured and optimized.